

Genetic Studies on Hypothalamus Functions
in Zebrafish

Ailani, Deepak

Doctor of Philosophy

Department of Genetics

School of Life Science

SOKENDAI (The Graduate University for
Advanced Studies)

Genetic Studies on Hypothalamus Functions in Zebrafish

Ailani, Deepak

Student ID: 20131801
Department of Genetics, SOKENDAI

Table of Contents

Summary	4
Introduction	7
Results	9
1. Genetic identification of hypothalamic neurons mediating locomotor activity in zebrafish larvae	9
1.1 Identification of the transgenic Gal4 lines labeling the hypothalamic area in larval zebrafish	9
1.2 Neuronal populations labeled in the 116A-gal4 and 1121A-gal4 lines are activated when fish perform tail-flips	10
1.3 Characterization of the 116A-gal4 and 1121A-gal4 lines	11
1.4 Functional imaging of the 116A-neurons in freely swimming zebrafish ...	12
1.5 Effect of inhibition of the 116A-neurons on locomotor activity	13
1.6 Effect of activation of the 116A-neurons on locomotor activity	15
2. Functional imaging of the 1121A-neurons at single-cell resolution	17
2.1 Activities of the hypothalamic 1121A-neurons during OMR	17
2.3 Tuning of activity of the hypothalamic 1121A-neurons to the speed of OMR stimulus	18
2.4 Activities of the 1121A telencephalic neurons during OMR	18

3. Activities of the 116A-neurons and 1121A-neurons in the cH in response to aversive stimuli	20
4. Immunohistochemistry of the 116A and 1121A neurons	22
Discussion	23
Materials and Methods	25
Acknowledgements	35
References	36

Summary

Locomotion is a rhythmic and alternating motor activity that allows an animal to move from one place to another, and is essential for survival of animals. In vertebrates, the hypothalamus has been shown to play an important role in regulation of locomotor activity. However, the functional circuits and cell populations mediating locomotor activity are still unclear. In this study, I aimed to investigate hypothalamic neuronal circuits and cell populations mediating locomotor activity using the model vertebrate zebrafish.

I performed a genetic screen using Tol2 transposon mediated gene trap and enhancer trap methods and generated transgenic fish that expressed Gal4 in specific brain regions in larval zebrafish. Then, I isolated a transgenic line named 116A that labeled a subpopulation of neurons in the caudal hypothalamus (cH), the intermediate hypothalamus (iH) and the paraventricular organ (PVO), and another line named 1121A that labeled a subpopulation of neurons in the cH, iH, PVO and the telencephalon. I performed calcium imaging using 116A-gal4;UAS:GCaMP6s and 1121A-gal4;UAS:GCaMP6s double transgenic fish, and found that the hypothalamic neurons labeled in these lines were activated when larval zebrafish performed spontaneous tail-flips. I hypothesized that those neuronal populations may regulate locomotor activity.

First, to test this hypothesis, I analyzed the activity of the neurons labeled in 116A (hereafter referred to as 116A-neurons) in freely swimming larvae after transfer to an imaging chamber. The locomotor activity of the larvae decreased gradually in the chamber, due to a process called habituation. I found that the activity of 116A-neurons also decreased during the habituation. To further investigate their functions, I inhibited the neural activities by crossing 116A-gal4 fish with the UAS-effector fish carrying the botulinum neurotoxin gene. The double transgenic fish showed reduced locomotor activity, and specifically reduced

swimming bout frequency. Then, I activated 116A-neurons by crossing 116A-gal4 fish with the UAS-effector fish carrying the rat TRPV1 cDNA, encoding an ion channel that is open in the presence of capsaicin, and found that the double transgenic fish showed increased locomotor activity after application of capsaicin. These indicated that the genetically tagged cH, iH, and PVO cells in the hypothalamus play a crucial role in regulating locomotor activity in zebrafish larvae.

Next, to further explore the function of hypothalamic neurons in locomotion, I analyzed the activity of neurons at single-cell resolution by using the 1121A-gal4 line, since expression levels of GCaMP6s in the 116A-gal4;UAS:GCaMP6s larvae were not strong enough for single-cell imaging. I set up a system for optomotor response (OMR) in which swimming behaviors are evoked in head restrained larvae upon onset of visual stimuli, namely moving black-and-red gratings, under a spinning-disk confocal microscope. I found that the cH and iH neurons in the 1121A line were activated synchronously upon onset of the OMR stimuli. Interestingly, when the grating speed was changed, the activity of the cH and iH neurons changed according to the grating speeds. To our knowledge, this is the first demonstration of tuning of hypothalamic activity to the speed of a moving visual stimulus. Also, I found that the activities of telencephalon neurons labeled in the 1121A line were increased upon onset of the OMR stimuli. Some of these activities were correlated with those observed in the hypothalamus, suggesting connection of these two areas.

Previous studies that employed c-fos and pERK staining to detect neuronal activation reported that aversive stimuli activated the caudal hypothalamic area in larval zebrafish. To determine if the hypothalamic neurons labeled in the 116A and 1121A lines are involved in this activity, I applied aversive stimuli, such as mustard oil and heat, to the transgenic larvae, and analyzed them by calcium imaging. I found that the neurons labeled in 116A and 1121A

lines were strongly activated by exposure to these aversive stimuli, suggesting that these neurons may be involved in aversive responses.

Finally, I performed immunohistochemistry, and showed that the 116A-neurons are mostly serotonergic. My present study provides a clue to understanding functions of a genetically identified neuronal population located in the caudal hypothalamus, the intermediate hypothalamus and the paraventricular organ in the larval zebrafish.

Introduction

The ability to move is crucial for the survival of an animal. Although there are many forms of locomotion such as walking, running, flying and swimming, all these forms employ a rhythmic and alternating motor activity that allows an animal to move from one place to another. Basic tasks such as food-seeking or escape from predators require precise modulation of locomotor activity. In vertebrates, a brain region called the hypothalamus has been shown to play an important role in regulation of locomotor activity (Jordan 1998). A study in decorticate cats showed that electrical activation of the hypothalamus evoked locomotor activity proportional to the strength of the activation, whereas ablation of the hypothalamus abolished all spontaneous locomotion (Shik et al. 1966). A study in freely moving rats, which used movable electrodes to electrically stimulate various hypothalamic sites, showed that activation of the lateral hypothalamus induced exploratory locomotion, while activation of the medial hypothalamus induced escape jumps (Lammers et al. 1988). A study in anesthetized rats showed that electrical and chemical activations of the perifornical and lateral hypothalamus evoked locomotor stepping (Sinnamon 1993). Although these studies demonstrated the involvement of the hypothalamus in regulating locomotion, the functional circuits and cell populations mediating locomotor activity were still unclear.

Zebrafish is a freshwater teleost fish and has been widely used as a model system to study the development and function of brain circuits (Engert & Wilson 2012). As a vertebrate, zebrafish has a brain structure similar to mammals. Several reports have suggested a homology between the mammalian and the fish hypothalamus. Functional homologs of the hypothalamic nuclei that mediate neuroendocrine response in mammals have been identified in zebrafish (Flik et al. 2006; Herget et al. 2014). Zebrafish also offers several powerful genetic tools such as the Gal4-UAS system. Our lab has developed *Tol2* transposon-mediated

gene trap and enhancer trap methods and we have generated transgenic fish lines that express Gal4 in specific tissues and organs, including specific neural populations in the brain (Asakawa et al. 2008; Kawakami et al. 2010). Also the Gal4-UAS system can be used to study the function of Gal4 expressing neurons by inhibiting their activity using genetically encoded neurotoxins such as tetanus toxin (Asakawa et al. 2008) and botulinum toxin (Sternberg et al. 2016). Furthermore, transparency of zebrafish at embryonic stages make them ideal for visualizing brain activities in live and behaving animals. Using genetically encoded calcium indicators, the Gal4-UAS system can be used to monitor the neural activity of Gal4 expressing neurons in intact and behaving zebrafish larvae (Muto et al. 2013; Muto & Kawakami 2016; Muto & Kawakami 2013; Muto et al. 2011).

In this study, I aimed to investigate hypothalamic neuronal circuits and cell populations mediating locomotor activity using the model vertebrate zebrafish. I isolated a transgenic zebrafish line named 116A that genetically tagged a neuronal population in the caudal hypothalamus (cH), the intermediate hypothalamus (iH) and the paraventricular organ (PVO). I showed that this neuronal population was mostly serotonergic and played a crucial role in mediating the locomotor activity of zebrafish larvae. I also isolated a transgenic line named 1121A that genetically tagged a neuronal population in the cH, iH, PVO and the telencephalon. By analyzing the activities of those neurons at single-cell resolution, I showed that the 1121A-neurons in the cH and iH were synchronously activated upon onset of a moving visual stimulus in head-restrained larvae. Furthermore, when the speed of moving stimulus was increased, the locomotor activity of the head restrained larvae and the activity of those cH and iH neurons also increased accordingly. I also showed that the activities of the telencephalic 1121A-neurons increased upon onset of the moving visual stimuli and some of these activities were correlated with those observed in the hypothalamus, suggesting a functional connection between these two areas.

Results

1. Genetic identification of hypothalamic neurons mediating locomotor activity in zebrafish larvae

1.1 Identification of the transgenic Gal4 lines labeling the hypothalamic area in larval zebrafish

Transgenic Gal4 zebrafish lines that label specific neural populations in the zebrafish brain at larval stages were created using gene trap and enhancer trap constructs (Kawakami et al. 2010) (described in Materials and Methods). Gal4 binds to the UAS sequence and activates transcription of genes located downstream of the UAS (Asakawa et al. 2008). These Gal4 fish were crossed with the UAS:GFP effector fish and the Gal4 expression patterns were visualized in the double transgenic larvae at 5 days post fertilization (dpf). I observed the GFP expression patterns in the brain of double transgenic larvae obtained from 608 Gal4 lines from the lateral side and identified 54 Gal4 lines that showed GFP expression in the hypothalamus of larval zebrafish. As examples, a list of 15 of the 54 lines is shown in Table 1. GFP expression patterns in the brain of the double transgenic larvae from these 15 lines are shown in Fig. 1.

Based on morphology and gene expression, four hypothalamic nuclei have been identified in the larval zebrafish brain, namely the rostral hypothalamus (rH), the intermediate hypothalamus (iH), the caudal hypothalamus (cH) and the inferior lobe of the hypothalamus (ILH) (Fig. 2A) (Mueller & Wullimann 2015; Rink & Guo 2004; Kaslin & Panula 2001). I analyzed transgenic Gal4 lines by using two-photon microscope, and identified Gal4 lines that labeled specific hypothalamic nuclei in larval zebrafish. I found that the transgenic lines named gSAIzGFFM116A, gSAIzGFFM1121A, and hspGFFDMC76A labeled

subpopulations of neurons in cH, iH and the paraventricular organ (PVO) (Fig. 2B), in cH, iH, PVO and the telencephalon (Fig. 2C), and in ILH (Fig. 2D), respectively.

1.2 Neuronal populations labeled in the 116A-gal4 and 1121A-gal4 lines are activated when fish perform tail-flips

I investigated the activities of the neuronal populations in gSAIzGFFM116A (hereafter referred to as 116A-gal4) and gSAIzGFFM1121A (hereafter referred to as 1121A-gal4) lines when larvae performed spontaneous tail-flips (Fig. 3). To visualize activities of neurons labeled by 116A-gal4 and 1121-gal4 lines (hereafter referred to as 116A-neurons and 1121A-neurons, respectively), I used the UAS-effector fish that carries the GCaMP6s gene (UAS:GCaMP6s fish). GCaMP is a genetically-encoded fluorescent calcium sensor, created from a fusion of GFP, calmodulin, and M13 peptide sequences (Nakai et al. 2001). GCaMP6s is a modified version of GCaMP that has an improved range of fluorescence signal and can detect single action potentials in neuronal somata (Chen et al. 2013). Activation of neurons increases the concentration of intra-cellular calcium which leads to an increase in GCaMP fluorescence. Thus, the level of GCaMP fluorescence is an indirect measure of neural activity.

I crossed the 116A-gal4 and 1121A-gal4 fish with the UAS:GCaMP6s fish. The double transgenic larvae were embedded in low melting agarose. The agarose around the tail was removed such that the tail was free to move but the head was fixed (head-restrained preparation). Activities of GCaMP6s in the head-restrained 116A-gal4; UAS:GCaMP6s and 1121A-gal4; UAS:GCaMP6s larvae were recorded using an epi-fluorescence microscope, while fish performed spontaneous tail-flips. I analyzed the GCaMP6s fluorescence intensity of the 116A-neurons (Fig. 3A) and 1121A-neurons in the cH, iH and PVO (Fig. 3B), and found that activities of those neurons increased significantly after initiation of tail-flips

compared to their spontaneous activities during the experiment. For the 116A-neurons, average dF/F_{min} during 10 s after initiation of tail-flips was 1.16 ± 0.11 while average dF/F_{min} during 10 s before initiation of tail-flips was 0.55 ± 0.10 ($n = 3$ fish, 38 tail-flips, $p < 10^{-4}$, paired t test) (Fig. 3C). For the 1121A-neurons in the cH, iH and PVO, average dF/F_{min} during 10 s after initiation of tail-flips was 0.53 ± 0.04 , while average dF/F_{min} during 10 s before initiation of tail-flips was 0.26 ± 0.04 ($n = 3$ fish, 31 tail-flips, $p < 10^{-4}$, paired t test) (Fig. 3D). I found that most of the individual tails flips were associated with the activation of 116A-neurons and 1121A-neurons. For 116A-gal4; UAS:GCaMP6s larvae, the total number of tail-flips during experiment was 38 and the tail-flips associated with activation of 116A-neurons was 37 (97%). For, 1121A-gal4; UAS:GCaMP6s larvae, the total number of tail-flips during experiment was 31 and the tail-flips associated with activation of 1121A-neurons was 26 (84%). These results suggested that activities of the 116A-neurons and 1121A-neurons (in cH, iH and PVO) were correlated with the motor activities. Based on this finding, I hypothesized that those neuronal populations may regulate locomotor activity of larval zebrafish.

1.3 Characterization of the 116A-gal4 and 1121A-gal4 lines

I extensively characterized the expression patterns of Gal4 in the 116A-gal4 and 1121A-gal4 lines. These Gal4 transgenic fish were crossed with the UAS:GFP fish and the GFP expression was analyzed in the double transgenic fish at larval and adult stages. I found that the 116A-gal4; UAS:GFP larvae showed GFP expression in neuronal populations in the cH, iH and PVO (Fig. 4A, 4B). GFP expression also revealed projections between the cells in the cH, iH and PVO (Fig. 4A, 4B). To determine Gal4 expression pattern in the 116A-gal4 line through development, I analyzed the GFP expression in the 116A-gal4; UAS:GFP larvae from 0 dpf to 4 dpf. I found that GFP expression was visible at 3 dpf, and the expression

pattern was already specific to the cH, iH and PVO (Fig. 4C). To determine the Gal4 expression pattern in the 116A-gal4 line at the adult stage, I analyzed the brain of an adult 116A-gal4; UAS:GFP fish and found that GFP expression was visible in the cH (Fig. 5A). Analysis of the 1121A-gal4; UAS:GFP larvae showed that GFP was expressed in neuronal populations in the cH, iH, PVO and the telencephalon (Fig. 6A). In the adult 1121A-gal4; UAS:GFP fish, GFP expression was visible in the cH and the telencephalon (Fig. 6B).

To determine the trapped genes or enhancers driving the expression of Gal4 in the 116A-gal4 and 1121A-gal4 lines, the Gal4 integration sites in the genome of these lines were characterized using inverse PCR. In the 116A-gal4 line, the transposon was integrated on chromosome 24, in the intronic sequences of two overlapping genes, *neurod6a* and *ccdc129* (Fig. 5B), and in the 1121A-gal4 line, the transposon was integrated in an intergenic region on chromosome 25 (Fig. 6C).

1.4 Functional imaging of the 116A-neurons in freely swimming zebrafish

To test the hypothesis that the 116A-neurons may mediate locomotor activity in larval zebrafish, I analyzed the activity of 116A-neurons in freely swimming larvae (Fig. 7A). The 116A-gal4; UAS:GCaMP6s larvae were placed in a rectangular imaging chamber and their locomotor activity and the GCaMP6s fluorescence were recorded for 30 minutes using an epi-fluorescence microscope.

To analyze the locomotor activity (total distance) of larvae in the imaging chamber, I calculated the X,Y co-ordinates of the fish (Fig. 7B). I analyzed the average total distance traveled by larvae during the 1st, 15th, and 30th minute after transfer to the imaging chamber, and found that the locomotor activity of the larvae decreased gradually over time. For the 1st, 15th and 30th minute, the total traveled distances were 10.1 ± 0.9 , 6.7 ± 0.3 , and 3.9 ± 0.2 ,

respectively (Fig. 8A). This was consistent with a previous study that showed that the locomotor activity of zebrafish larvae gradually decreases after transfer to another apparatus, before reaching a relatively stable baseline level. This process is called ‘habituation’ (Yokogawa et al. 2012).

To analyze the GCaMP6s fluorescence in the 116A-neurons during the 1st, 15th and 30th minute after transfer to the imaging chamber, I performed image registration (Fig. 7B). I found that the activity of the 116A-neurons decreased gradually over time after transfer to the imaging chamber. For the 1st, 15th and 30th minute, the dF/F_{min} were 3.9 ± 0.2 , 2.3 ± 0.1 , and 0.55 ± 0.05 , respectively (Fig. 8B). This suggested that the activity of the 116A-neurons was correlated with the locomotor activity in the freely swimming fish during habituation.

1.5 Effect of inhibition of the 116A-neurons on locomotor activity

To investigate the role of the 116A-neurons in regulation of locomotor activity in larval zebrafish, I genetically inhibited their neural activity using the UAS-effector fish that carries a codon-optimized botulinum neurotoxin gene fused with the GFP sequence (UAS:BoTx:GFP fish). Expression of this neurotoxin was shown to efficiently inhibit neural activity in larval zebrafish by abolishing synaptic release of neurotransmitter without triggering off-target effects (Sternberg et al. 2016). I crossed the 116A-gal4 fish with the UAS:BoTx:GFP fish and analyzed the locomotor activity of the double transgenic fish at 5 dpf. Expression of BoTx:GFP in the 116A-gal4; UAS:BoTx:GFP larvae was strong enough to be visible under a fluorescence stereomicroscope (Fig. 9). I put individual 116A-gal4; UAS:BoTx:GFP larvae and their control siblings in individual wells of a multi-well plate and recorded their locomotor activity for 90 minutes. After recording, I analyzed the locomotor activity and found that the locomotor activity of the 116A-gal4; UAS:BoTx:GFP larvae was

significantly lower than their control siblings. For the 116A-gal4; UAS:BoTx:GFP larvae, the total distance traveled during 90 minutes was 462.4 ± 63.5 pixels, while for the control larvae, the total distance traveled was 699.5 ± 81.6 pixels (Fig. 10A). This suggested that the 116A-neurons played an important role in regulation of locomotor activity in zebrafish.

Since zebrafish larvae swim in discrete units called bouts, the locomotor activity of a freely swimming larva can be mathematically decomposed into bout frequency and bout distance:

$$\text{Locomotor activity (total distance)} = \text{Bout frequency} * \text{Bout distance}$$

To know which of these two parameters were affected in the 116A-gal4; UAS:BoTx:GFP larvae, I analyzed the bout frequency and bout distance for the 90 minutes in multi-well plate. I found that the average bout frequency of the 116A-gal4; UAS:BoTx:GFP larvae was significantly lower than that of their control siblings. For the 116A-gal4; UAS:BoTx:GFP larvae, the average bout frequency during 90 minutes was 30.8 ± 4.8 bouts per minute, while for the control larvae, the average bout frequency was 46.1 ± 5.7 bouts per minute (Fig. 10B). Interestingly, there was no significant difference in the average bout distance between the 116A-gal4; UAS:BoTx:GFP larvae and their control siblings. For the 116A-gal4; UAS:BoTx:GFP larvae, the average bout distance during 90 minutes was 17.2 ± 1.4 pixels, while for the control larvae, the average bout distance was 16.8 ± 1.1 pixels (Fig. 10C). This suggested that inhibition of the 116A-neurons specifically reduced the bout frequency of larval zebrafish.

I also performed a control experiment to test the effect of the botulinum neurotoxin transgene alone (without any Gal4) on the locomotor activity. I crossed the UAS:BoTx:GFP fish with wildtype (WT) fish and recorded the locomotor activity of the 5 days old UAS:BoTx:GFP and their WT siblings for 60 minutes in a multi-well plate. After the recording, I identified the UAS:BoTx:GFP larvae and their WT siblings using PCR-based

genotyping and analyzed their locomotor activities. I found that locomotor activity of the UAS:BoTx:GFP larvae did not differ significantly from their WT siblings. For UAS:BoTx:GFP larvae, the average distance during 60 minutes was 604.3 ± 53.7 pixels, and for the WT larvae, the average distance was 602.1 ± 85.9 pixels (Fig. 11). Hence, the presence of botulinum neurotoxin transgene alone did not have an effect on the locomotor activity of the larvae.

1.6 Effect of activation of the 116A-neurons on locomotor activity

Next, to determine if the activity of the 116A-neurons could drive locomotor activity of zebrafish larvae, I tested the effect of activation of the 116A-neurons on the locomotor activity of larval zebrafish. A recent study reported the use of genetically-encoded rat TRPV1 channel and capsaicin to activate neurons in freely swimming zebrafish larvae (Chen et al. 2015). Mammalian TRPV1 channels, including the rat TRPV1, are activated by application of capsaicin (Caterina et al. 1997), whereas the zebrafish TRPV1 ortholog is insensitive to capsaicin (Gau et al. 2013). Hence, to specifically activate the Gal4-labeled neurons in freely swimming zebrafish larvae, I and another lab member generated a UAS-effector fish carrying the codon optimized rat TRPV1 cDNA (UAS:TRPV1 fish).

I crossed the 116A-gal4 fish with the UAS:TRPV1 fish and recorded the locomotor activity of 5 days old double transgenic larvae and their control siblings for 5 hours in a multi-well plate in presence of 10 μ M capsaicin. This concentration of capsaicin was shown to robustly activate TRPV1-expressing neurons in the brains of freely swimming zebrafish larvae without non-specific effects on their locomotor activity (Chen et al. 2015). After the recording, I identified the 116A-gal4; UAS:TRPV1 larvae and their control siblings using PCR-based genotyping and analyzed their locomotor activities. I found that the locomotor

activity of the 116A-gal4; UAS:TRPV1 larvae was significantly higher than their control siblings between 1.5 hours to 3.5 hours after incubation in 10 μ M capsaicin ($p < 0.05$) (Fig. 12A).

To know which bout parameters were affected in the 116A-gal4; UAS:TRPV1 larvae in presence of capsaicin, I analyzed the bout frequency and bout distance during swimming for 5 hours in presence of capsaicin. I found that the average bout frequency of the 116A-gal4; UAS:TRPV1 larvae was significantly higher than that of control siblings between 1.5 hours to 3.5 hours after incubation in 10 μ M capsaicin ($p < 0.05$) (Fig. 12B). Interestingly, there was no significant difference in the average bout distance between the 116A-gal4; UAS:TRPV1 larvae and their control siblings (Fig. 12C). This suggested that activation of the 116A-neurons specifically increased the bout frequency of larval zebrafish.

2. Functional imaging of the 1121A-neurons at single-cell resolution

2.1 Activities of the hypothalamic 1121A-neurons during OMR

To further explore the activity of the hypothalamic neurons, I analyzed the activity of the 1121A-neurons at single-cell resolution. For this experiment, I used the 1121A-gal4; UAS:GCaMP6s fish, since the GCaMP6s expression level in the 116A-gal4; UAS:GCaMP6s larvae was not strong enough for single-cell imaging (Fig. 13A, 13B).

I set up a system for optomotor response (OMR) in which swimming behavior is evoked in head-restrained larvae upon onset of a moving visual stimulus, namely moving black and red gratings (Severi et al. 2014). Head-restrained larvae were presented with moving gratings from below using an LED projector, while their tail movements were captured using a high speed IR camera and the GCaMP6s fluorescence in the brain was recorded at single-cell resolution using a spinning-disk confocal microscope (Fig. 13C).

I presented the 5 days old head-restrained 1121A-gal4; UAS:GCaMP6s larvae with 10 seconds of static gratings followed by 10 seconds of moving gratings at speed of 30 mm/s. This speed of moving gratings elicits robust swimming behavior in head-restrained larvae (Severi et al. 2014). I analyzed the GCaMP6s fluorescence intensity of the 1121A-neurons at single-cell resolution and found that the activities of the 1121A-neurons in the cH and iH were synchronous, and increased upon onset of the moving gratings (Fig. 14).

2.3 Tuning of activity of the hypothalamic 1121A-neurons to the speed of OMR stimulus

A previous study showed that when the speed of moving gratings is increased in the OMR system, the locomotor activity of the head-restrained larvae also increases accordingly (Severi et al. 2014). I investigated the activities of the hypothalamic 1121A-neurons while presenting moving gratings at six different speeds (0.5, 1, 5, 10, 15, or 30 mm/s). These six grating speeds were shown to evoke a graded locomotor response in head-restrained zebrafish larvae (Severi et al. 2014). I found that increasing the grating speed increased the bout frequency of the head restrained 1121A-gal4; UAS:GCaMP6s larvae ($R^2 = 0.69$) (Fig. 15A), which is consistent with the previous study (Severi et al. 2014). Interestingly, analysis of the GCaMP6s fluorescence intensity of the 1121A-neurons in the cH and iH showed that activities of those neurons increased with the increasing grating speeds (left hemisphere: $R^2 = 0.73$, right hemisphere: $R^2 = 0.78$) (Fig. 15B). This suggested that the activity of hypothalamic 1121A-neurons was tuned to the speed of the moving gratings.

2.4 Activities of the 1121A telencephalic neurons during OMR

Since the 1121A; UAS:GCaMP6s larvae also expressed GCaMP6s in a population of neurons in the telencephalon (Fig. 14A), I analyzed the activities of telencephalic 1121A-neurons using the OMR system. I found that activities of several telencephalic 1121A-neurons increased upon onset of moving gratings (Fig. 16). Some of these activities were correlated with those observed in the hypothalamic 1121A-neurons (Fig. 16), suggesting a functional connection between these two areas.

I analyzed the projections of the telencephalic 1121A-neurons using the UAS:ChRWR:GFP fish. ChRWR (Channelrhodopsin wide receiver) is a membrane ion

channel and for unknown reason, the UAS:ChRWR:GFP fish showed sparse expression of ChRWR:GFP in the telencephalon of the 1121A-gal4; UAS:ChRWR:GFP; UAS:RFP larvae. Some of the 1121A-gal4; UAS:ChRWR:GFP; UAS:RFP larvae expressed ChRWR:GFP in a small subset of neurons in the telencephalon with almost no expression in the hypothalamus area, thus making it possible to trace the projections of these telencephalic neurons. I analyzed the brains of those larvae using two-photon microscope and found that the ChRWR:GFP-expressing telencephalic neurons extended projections that innervated the hypothalamus area (Fig. 17). This finding suggested an anatomical connection between the telencephalon and the hypothalamus in zebrafish larvae.

3. Activities of the 116A-neurons and 1121A-neurons in the cH in response to aversive stimuli

Previous studies that employed c-fos and pERK staining to detect neuronal activation reported that aversive stimuli activated a genetically unidentified population of neurons in the cH (Semenova et al. 2014; Randlett et al. 2015). To investigate if the 116A and 1121A-neurons were activated by aversive stimuli, I analyzed the neural activity after application of aversive stimuli, namely mustard oil and hot water (Randlett et al. 2015; Prober et al. 2008).

I crossed the 116A-gal4 fish with the UAS:GCaMP6s fish and embedded the 5 days old 116A-gal4; UAS:GCaMP6s double transgenic larvae in low melting agarose. The agarose from around the tail and in front of the head was removed such that the tail and the front of the head were exposed. I used an automated perfusion system to first deliver the vehicle solution (DMSO or 28°C water) and then deliver the aversive stimulus (mustard oil or 37°C water), while recording the GCaMP6s fluorescence in the 116A-neurons using an epi-fluorescence microscope (Fig. 18A). I analyzed the GCaMP6s fluorescence intensity in the 116A-neurons and found that activities of 116A-neurons in the cH did not change significantly after application of vehicle (dF/Fmin during 1 minute before adding DMSO = 0.66 ± 0.07 , during 1 minute after adding DMSO = 0.96 ± 0.24 , $n = 3$, $P = 0.29$, paired t test) (dF/Fmin during 1 minute before adding 28°C water = 0.58 ± 0.22 , during 1 minute after adding 28°C water = 0.55 ± 0.31 , $n = 3$, $P = 0.79$, paired t test). Activities of 116A-neurons in the cH significantly increased after application of aversive stimuli (dF/Fmin: during 1 minute before adding mustard oil = 0.73 ± 0.12 , during 1 minute after adding mustard oil = 2.16 ± 0.30 , $n = 3$, $P = 0.02$, paired t test) (dF/Fmin: during 1 minute before adding 37°C water = 0.44 ± 0.22 , during 1 minute after adding 37°C water = 2.44 ± 0.41 , $n = 3$, $P = 0.01$, paired t test) (Fig. 18B, 18C).

Using the same experimental system, I analyzed the activities of the 1121A-neurons before and after application of DMSO (vehicle) and mustard oil. I found that activities of 1121A-neurons in the cH did not significantly change after application of DMSO (dF/Fmin: during 1 minute before adding DMSO = 0.32 ± 0.09 , during 1 minute after adding DMSO = 0.44 ± 0.02 , $n = 3$, $P = 0.28$, paired t test) (Fig. 19B). Activities of 1121A-neurons in the cH significantly increased after application of mustard oil (dF/Fmin: during 1 minute before adding mustard oil = 0.49 ± 0.12 , during 1 minute after adding mustard oil = 1.22 ± 0.17 , $n = 3$, $P = 0.004$, paired t test) (Fig. 19B). Hence, the 116A-neurons and 1121A-neurons may also be involved in the aversive responses.

4. Immunohistochemistry of the 116A and 1121A neurons

It has been shown that the zebrafish cH, iH and PVO are rich in serotonergic neurons (Kaslin & Panula 2001; Rink & Guo 2004). I analyzed the GFP-positive cells in the 116A-gal4; UAS:GFP larvae at 5 dpf by double immunostaining using the anti-GFP and anti-5-HT (serotonin) antibodies (Fig. 20A). I found that most of the GFP-positive cells in the cH, iH and PVO were serotonin-positive (GFP⁺ cells that were 5-HT⁺ : cH = 89% ± 1.4% (408 cells/ 458 cells), iH = 90% ± 0.3% (91 cells/ 101 cells), PVO = 88% ± 6.1% (49 cells/ 55 cells), n = 2 fish), indicating that most of the 116A-neurons were serotonergic. I also analyzed the number of serotonin-positive cells that were GFP-positive. Results indicated that a subpopulation of serotonergic neurons were labeled by the 116A-gal4 line (5-HT⁺ cells that were GFP⁺ : cH = 61% ± 5% (306 cells/ 502 cells), iH = 67% ± 8% (77 cells/ 116 cells), PVO = 40% ± 9% (66 cells/ 136 cells), n = 2 fish).

I analyzed the cells in the 1121A-gal4; UAS:GFP larvae at 5 dpf by double immunostaining using the anti-GFP and anti-5-HT antibodies (Fig. 20B), and found that almost all of the serotonin-positive cells in the cH, iH and PVO were also GFP-positive (5-HT⁺ cells that were GFP⁺ : cH = 100% ± 0% (700 cells/ 700 cells), iH = 100% ± 0% (178 cells/ 178 cells), PVO = 99% ± 0.6% (170 cells/ 172 cells), n = 3 fish). This indicated that most of the serotonergic neurons were labeled by the 1121A-gal4 line. I also observed that several GFP-positive cells were not labeled by anti-5-HT antibody, indicating that the 1121A-gal4 line may also include other types of cells which are not serotonergic.

Discussion

Although the hypothalamus has been shown to play an important role in regulation of locomotor activity (Jordan 1998; Shik et al. 1966; Lammers et al. 1988; Sinnamon 1993), the functional circuits and cell populations of hypothalamus mediating locomotor activity are still unclear. In this study, I took a genetic approach using zebrafish to investigate hypothalamic neuronal circuits and cell populations mediating locomotor activity.

I isolated the transgenic zebrafish line named 116A that genetically tagged a neuronal population in the cH, iH and PVO. I showed that this neuronal population was mostly serotonergic and played a crucial role in mediating the locomotor activity of zebrafish larvae. Serotonergic neurons have been found in the hypothalamus of several non-placental vertebrate species, including zebrafish (Lillesaar 2011; Gaspar & Lillesaar 2012). In the placental mammals, serotonergic neurons were found to be absent from the hypothalamus and were observed exclusively in the raphe nuclei (Dahlström & Fuxe 1964; Jacobs & Azmitia 1992), indicating that the mammalian serotonergic system is an exception.

Previous studies have shown that the zebrafish cH, iH and PVO also contain dopaminergic neurons (Kaslin & Panula 2001; Rink & Guo 2004; Semenova et al. 2014). A recent study showed that a subpopulation of these dopaminergic neurons, which were labelled by a transgenic zebrafish line using 9.6 kb of sequence upstream of *th2* gene that encodes tyrosine hydroxylase, may also be involved in mediating locomotor activity of zebrafish larvae (McPherson et al. 2016). The serotonergic and dopaminergic neuronal populations in the cH, iH and PVO form the diencephalic cerebrospinal fluid (CSF)-contacting periventricular neurons that have been found in all vertebrates except mammals (Rink & Wullmann 2001; Rink & Guo 2004; Kaslin & Panula 2001). These neurons may release the neurotransmitters into the CSF to activate potential downstream targets. This

could explain the slow response of locomotor activity of the 116A-gal4; UAS:TRPV1 larvae upon application of the capsaicin (Fig. 12).

I also isolated the transgenic line named 1121A that genetically tagged a neuronal population in the cH, iH, PVO and the telencephalon. I showed that this neuronal population included most of the serotonergic neurons in the cH (100%), the iH (100%) and the PVO (99%) and non-serotonergic cells as well. By analyzing the activities of those neurons at single-cell resolution, I showed that the 1121A-neurons in the cH and iH were synchronously activated upon onset of a moving visual stimulus that evokes swimming behaviors in head-restrained larvae. Furthermore, when the speed of moving stimulus was increased, the locomotor activity of the head restrained larvae and the activity of the 1121A neurons also increased accordingly. To my knowledge, this is the first demonstration of tuning of the activity of the hypothalamic neurons to the speed of a moving visual stimulus.

Little was known about the neural activities and functions of the telencephalon neurons during locomotion in zebrafish larvae. I showed that the activities of the telencephalic 1121A-neurons increased upon onset of the moving visual stimuli, and some of these activities were correlated with those observed in the hypothalamus, suggesting a functional connection between these two areas.

Thus, my present study provided clues to understanding functions of a genetically identified neuronal population located in the caudal hypothalamus, the intermediate hypothalamus and the paraventricular organ in mediating the locomotor activity of the larval zebrafish.

Materials and Methods

Zebrafish husbandry and preparation of larvae for imaging and behavioral studies

Zebrafish (*Danio rerio*) were maintained in accordance with the Guide for the Care and Use of Laboratory Animals of the Institutional Animal Care and Use Committee (IACUC, approval identification number 27-2). Adult zebrafish were maintained at 25°C under a regular 13/11 hour light/dark cycle. Zebrafish larvae were reared on a 12/12 hour light/dark cycle at 28°C in E3 medium unless otherwise stated.

Generation of transgenic zebrafish

Transgenic fish expressing Gal4 were generated by the gene trap and enhancer trap methods described in Asakawa et al. 2008 and below.

Micro-injection and excision assay

Transposase mRNA was synthesized in vitro as described previously (Kawakami et al. 2004). Approximately 1 nl of construct-mRNA containing 25 ng/uL of circular DNA of a transposon donor plasmid (DNA construct) and mRNA were co-injected into fertilized eggs at single cell stage. To check integration of the construct in zebrafish genome, approximately 10 hours after the injection, DNA sample was prepared from the embryos and excision assay was performed (Kawakami & Shima 1999; Kawakami et al. 2004).

Identification of transgenic fish with specific Gal4 expression patterns

GFP expression patterns in the brain of 1 day and 5 days old double transgenic embryos obtained from injected founder fish were observed under a fluorescence stereomicroscope (Leica, MZ16FA) and images were captured using DFC300 FX camera (Leica Microsystems). Images were captured from both the dorsal and lateral sides of the embryos.

Identification of loci of insertions in transgenic fish

Fish with single Tol2 insertion were identified using Southern blot hybridization (Kawakami et al. 2004). Using inverse PCR and linker mediated PCR techniques, the site of insertion of the Tol2 construct was identified. The standard protocols previously described (Kawakami et al. 2004; Kotani et al. 2006; Urasaki et al. 2006) were used for the characterization.

Tol2-based Gal4 constructs

The Gal4 gene is a fusion of DNA binding domain from Gal4 and two transcription activation modules of VP16 (2xPADALDDFDLDMML) (Asakawa et al. 2008).

The details of individual enhancer/gene trap Gal4 constructs used to create transgenic fish is as follows:

T2KhspGFFDMC – An enhancer trap construct containing two splice acceptors from rabbit β -globin gene, two SV40 ployA signal, hsp70 promoter region and Gal4 gene between essential cis-sequences of Tol2.

T2HhspzGFFgDMC – An enhancer trap construct containing two splice acceptors from rabbit β -globin gene, two SV40 ployA signal, hsp70 promoter region and Gal4 gene between essential cis-sequences of Tol2.

T2KSAGFF(LF) – An enhancer trap construct containing a splice acceptor from rabbit β -globin gene, Gal4 gene and SV40 ployA signal between essential cis-sequences of Tol2.

T2GgSA2AzGFF – An enhancer trap construct containing a splice acceptor from rabbit β -globin gene, flag-tag, 2A peptide sequence, Gal4 gene and SV40 ployA signal between essential cis-sequences of Tol2.

T2GgSAIzGFFD – A gene trap construct containing a splice acceptor from rabbit β -globin gene, IRES sequence, Gal4 gene, SV40 ployA signal and FRT sequences between essential cis-sequences of Tol2.

T2GgSAIzGFFM – A gene trap construct containing a splice acceptor from rabbit β -globin gene, IRES sequence, Gal4 gene, SV40 ployA signal, 4xMAZ transcription termination site and FRT sequences between essential cis-sequences of Tol2.

Tol2 based UAS constructs

T2KUASGFP – Construct containing 5xUAS, TATA sequence, the EGFP gene, and the SV40 polyA between essential cis-sequences of Tol2. This UAS:GFP line was used to visualize pattern of Gal4 expressing cells and tissues in the zebrafish larvae and adult.

T2SUASzBoTxBLCGFP – Construct containing 5xUAS, TATA sequence, the codon optimized botulinum toxin B light chain gene (Kurazono et al. 1992) fused to the EGFP gene, and the SV40 polyA between essential cis-sequences of Tol2 .

T2UASzTRPV1mCherry – Construct containing 5xUAS, TATA sequence, codon optimized TRPV1 (rat) gene fused to mCherry gene, and the SV40 polyA between essential cis-sequences of Tol2.

T2UASChRWRGFP – Construct containing 14xUAS, Channelrhodopsin-wide receiver gene (Umeda et al. 2013) fused to EGFP gene, cloned into pT2AL200R150G (Kawakami et al. 2004; Urasaki et al. 2006).

UAS:GCaMP6s – Construct containing 5xUAS, the heat shock protein 70 promoter (650 bp), a zebrafish codon-optimized GCaMP6s (Chen et al. 2013), and the SV40 polyA between essential cis-sequences of Tol2.

Examination of gal4 expression patterns using a fluorescence stereomicroscope

Transgenic zebrafish larvae on a nacre background or with 1-phenyl 2-thiourea - treatment were anaesthetized using tricaine and observed under a Leica MZ16FA fluorescence stereomicroscope.

Examination of gal4 expression patterns using a two-photon laser confocal microscope

Transgenic zebrafish larvae on a nacre background or with 1-phenyl 2-thiourea - treatment were anaesthetized using tricaine and observed under a Zeiss LSM7MP microscope using the Z-stack function.

Behavior assay system to measure locomotor activity of the larval zebrafish

Individual 5 day old zebrafish larvae were transferred to individual wells of a 24 well multi-well plate containing 500 µl water. The plate was kept on top of an infrared (IR) LED

panel and larvae were habituated for 2 hours. Locomotion of larvae was recorded from top using an IR sensitive camera (Ximea). X, Y co-ordinates of the larvae were analyzed using ImageJ.

Swim kinematics analysis

The instant speed of the larvae was calculated by subtracting the displacement in the consecutive frames. A cutoff value was empirically determined and set at one pixel per frame to detect frames in which fish was moving. Based on the slope of the speed of the larvae, start and end of swim bouts were detected and bout frequency was calculated. Average bout distance was calculated by dividing the total distance with the bout frequency.

Establishment of a new UAS:BoTx:GFP line with strong neurotoxin expression

UAS:BoTx:GFP construct was injected at single cell stage and the founder fish were screened for the presence of UAS:BoTx:GFP. hspGFF3B line was used for the founder screen as it had strong Gal4 expression in muscle at 1 dpf (Fig. 21A). Expression strength of UAS:BoTx:GFP insertions from founders was quantified both visually and programmatically using ImageJ software. The result of the founder screen is shown in Table 2. Total 27 founders were screened using hspGFF3B line and 16 founders produced offspring with visible expression of UAS:BoTx:GFP. The strength of UAS:BoTx:GFP expression was characterized in the offspring both visually and using ImageJ software (Table 2) (Fig. 21B-F). Visually, the expression level of UAS:BoTx:GFP in an embryo was characterized in the increasing order of strength as ‘Weak’, ‘Medium’ or ‘Strong’. Using ImageJ software, the expression level of UAS:BoTx:GFP in an embryo was characterized in the increasing order of strength as ‘Class 1’ (weakest) to ‘Class 5’(strongest). 4 founders whose offspring had

Class 5 level of expression of UAS:BoTx:GFP expression were used for further mating and establishment of stable transgenic line of UAS:BoTx:GFP, and only one of the four founders produced healthy offspring with strong expression of UAS:BoTx:GFP in the subsequent generations (Table 2). The offspring were analyzed using Southern blot to identify the ones with single insertion of UAS:BoTx:GFP construct and strong expression.

Calcium imaging in head restrained larvae

For the imaging of an agarose-embedded larva, a single larva was mounted in 2% low melting agarose. Agarose around the tail was removed to make space for tail to move. Time-lapse recording was performed with an acquisition rate of 5 fps. Chemicals were delivered using a perfusion system. MATLAB and DAQ device was used to generate trigger voltage to simultaneously control the valve and the CMOS camera (ORCA-Flash4.0, model:C11440-22CU, Hamamatsu Photonics, Hamamatsu, Japan). ImageJ was used to obtain mean pixel values (i.e. calcium signals) in a region of interest (ROI) set on a brain structure in the time-lapse movie. Calcium signals were presented as normalized GCaMP6s fluorescence intensity (dF/F_{min}). F_{min} (minimum fluorescence intensity during the recording session) was subtracted from the GCaMP6s fluorescence intensities (mean pixel values in a ROI set on the cH, iH, PVO or other neuronal structures), and the remainder was divided by F_{min} to obtain dF/F_{min} .

Calcium imaging in freely swimming larvae

GCaMP6s was expressed in the larval brain by mating Gal4 fish with UAS:GCaMP6s transgenic zebrafish. To image calcium activity, a single free-swimming larva was put in a small rectangular chamber (Secure-Seal Hybridization Chamber Gasket, 25 mm length x 5

mm width x 0.8 mm depth) and observed under an epi-fluorescence microscope (Imager.Z1, Carl Zeiss, Germany) with an objective lens (2.5X/NA0.12 or 5X/NA0.15) equipped with a scientific CMOS camera (ORCA-Flash4.0, model:C11440-22CU, Hamamatsu Photonics, Hamamatsu, Japan). Images were recorded at 20 fps (50 ms exposure). The XY-stage was occasionally manually moved to locate the larva at the center of the camera view. Fluorescence images were acquired with time-lapse recording software (HCImage with a Hard Disk Recording module, Hamamatsu Photonics, Japan). ImageJ was used to obtain mean pixel values (i.e. calcium signals) in a ROI set on a brain structure in the time-lapse movie. Calcium signals were presented as normalized GCaMP6s fluorescence intensity (F/F_{min}). GCaMP6s fluorescence intensities (mean pixel values in a ROI set on the cH, ILH, PVO or other neuronal structures) divided by F_{min} (minimum fluorescence intensity during the recording session).

Calcium imaging with a confocal microscope

The confocal laser scanning microscope system used for calcium imaging consisted of a microscope (Examiner, Carl Zeiss, Germany), a scanning unit with a Nipkow spinning disk (CSU-W1, Yokogawa Electric, Tokyo, Japan) and an EM-CCD camera (iXon DU- 888, Andor, Belfast, UK). The imaging system was controlled by iQ3 software (Andor, Belfast, UK). A water immersion objective lens (W Plan-Apochromat 20X/1.0, Carl Zeiss, Germany) was used.

Presentation of OMR stimulus for calcium imaging while recording tail movement

Trials 20 s long were separated by 120 s inter-trial intervals during which the grating was static. The grating speeds (0.5, 1, 5, 10, 15, or 30 mm/s) were presented four times. The

tail was illuminated with IR LEDs from below and the tail movement was recorded using an IR sensitive camera (Ximea) at 60fps. Tail motion was detected using ROI based analysis of the pixel values using ImageJ.

Analysis of calcium activity at single cell resolution

The neural activity in 1121A-gal4; UAS:GCaMP6s fish was analyzed at single-cell resolution using the Constrained Non-negative Matrix Factorization (CNMF) algorithm (Pnevmatikakis et al. 2016). CNMF expresses the spatiotemporal calcium fluorescence activity as the product of a spatial matrix that encodes the spatial footprint of each neuron in the optical field and a temporal matrix that characterizes the calcium concentration of each neuron over time. In terms of segmenting and extracting time course from calcium imaging data, this algorithm performs better than the traditionally used PCA/ICA algorithm (Mukamel et al. 2009; Pnevmatikakis et al. 2016). The CNMF algorithm was used to identify the locations of individual neurons, demix spatially overlapping components, and denoise and deconvolve the neural activity from the slow dynamics of GCaMP6s. CNMF was initialized using an efficient Greedy method with 100 independent components that explained significant percent of variance observed in data (Fig. 29B). These 100 spatial components were then refined by Hierarchical Alternating Least Squares (HALS) method which grouped the regions that were spatially close and showed correlated temporal activities. This resulted in identification of several independent components (Fig. 29C). All the neurons in cH and iH were grouped as a single independent component (Fig. 29C), indicating that all identifiable neurons in cH and iH showed similar patterns of activities during fictive swimming.

Standard cluster analysis using pairwise correlations was performed to group telencephalon components displaying similar responses during OMR.

Immunohistochemistry

Immunohistochemistry was performed as described in (Randlett et al. 2015). Five days old 1-phenyl 2-thiourea – treated embryos were fixed in 4% paraformaldehyde (PFA) in phosphate-buffered saline (PBS) +0.25% Triton (PBT) overnight at 4°C, washed with PBT and then incubated in 150 mM TrisHCl pH 9.0 for 15 minutes at 70°C. Then, the samples were washed with PBT and incubated in 0.05% Trypsin-EDTA on ice. Then, the samples were washed with PBT and treated for 1 hour at room temperature in blocking buffer 2% normal goat serum, 1% bovine serum albumin (BSA), 1% DMSO, and then incubated at 4°C overnight with primary antibodies diluted in 1% BSA, 1% DMSO in PBT. Then, the samples were washed with PBT and incubated at 4°C overnight with secondary antibodies diluted in 1% BSA, 1% DMSO in PBT. Then, the samples were washed with PBT and mounted in low melting agarose and observed under a Zeiss LSM7MP microscope using the Z-stack function.

The following primary antibodies were used in this study: mouse anti-GFP (1:1000 dilution, Chemicon) and rabbit anti-5HT (1:1000 dilution, Sigma, S5545). The following secondary antibodies were used in this study: goat anti-mouse Alexa 488 (1:1000 dilution, Invitrogen, A11001) and goat anti-rabbit Alexa Fluor 546 (1:1000 dilution, Invitrogen, A11008). Images were processed using ImageJ (Schneider et al. 2012).

Statistical Analysis

All data are presented as mean \pm SEM and all error bars denote standard error mean (SEM). Unpaired *t* test was used to compare means from experimental groups of interest. Paired *t* test was used to compare means from an experimental group at different time points or different stimulus intensities. Two-tailed P values were calculated and P values less than

0.05 were considered significant. Correlation was analyzed by calculating R^2 values through linear curve fitting (linear regression) in MS Excel. No data points were excluded in this study. Number of animals is denoted by n. Statistical analysis was performed using GraphPad software.

Acknowledgements

I acknowledge my academic supervisor, Dr. Koichi Kawakami, for his advice and guidance, and all the Kawakami lab members for their immense help and support. I thank Dr. Hidenobu Mizuno for helping me with the two-photon microscope. I also acknowledge the members of my progress committee: Dr. Takuji Iwasato, Dr. Tatsumi Hirata, Dr. Jun Kitano, and Dr. Tsuyoshi Koide, for their advice and guidance. I am also grateful to Dr. Hiromi Hirata for constructive discussions and helpful feedback. Finally, I acknowledge Sokendai and NIG for its valuable support.

References

- Asakawa, K. et al., 2008. Genetic dissection of neural circuits by Tol2 transposon-mediated Gal4 gene and enhancer trapping in zebrafish. *Proceedings of the National Academy of Sciences*, 105(4), pp.1255–1260.
- Caterina, M.J. et al., 1997. The capsaicin receptor: a heat-activated ion channel in the pain pathway. *Nature*, 389(6653), pp.816–824.
- Chen, S. et al., 2015. TRP channel mediated neuronal activation and ablation in freely behaving zebrafish. *Nature Methods*, 13(2), pp.147–150.
- Chen, T.-W. et al., 2013. Ultrasensitive fluorescent proteins for imaging neuronal activity. *Nature*, 499(7458), pp.295–300.
- Dahlström, A. & Fuxe, K., 1964. Localization of monoamines in the lower brain stem. *Experientia*, 20(7), pp.398–9.
- Engert, F. & Wilson, S., 2012. Zebrafish neurobiology: From development to circuit function and behaviour. *Developmental Neurobiology*, 72(3), pp.215–217.
- Flik, G. et al., 2006. CRF and stress in fish. *General and Comparative Endocrinology*, 146(1), pp.36–44.
- Gaspar, P. & Lillesaar, C., 2012. Probing the diversity of serotonin neurons. *Philosophical Transactions of the Royal Society of London B: Biological Sciences*, 367(1601).
- Gau, P. et al., 2013. The zebrafish ortholog of TRPV1 is required for heat-induced locomotion. *The Journal of neuroscience : the official journal of the Society for Neuroscience*, 33(12), pp.5249–60.

- Herget, U. et al., 2014. Molecular neuroanatomy and chemoarchitecture of the neurosecretory preoptic-hypothalamic area in zebrafish larvae. *Journal of Comparative Neurology*, 522(7), pp.1542–1564.
- Jacobs, B.L. & Azmitia, E.C., 1992. Structure and function of the brain serotonin system. *Physiological Reviews*, 72(1).
- Jordan, L.M., 1998. Initiation of Locomotion in Mammals. *Annals of the New York Academy of Sciences*, 860(1 NEURONAL MECH), pp.83–93.
- Kaslin, J. & Panula, P., 2001. Comparative anatomy of the histaminergic and other aminergic systems in zebrafish (*Danio rerio*). *The Journal of comparative neurology*, 440(4), pp.342–77.
- Kawakami, K. et al., 2004. A Transposon-Mediated Gene Trap Approach Identifies Developmentally Regulated Genes in Zebrafish. *Developmental Cell*, 7(1), pp.133–144.
- Kawakami, K. et al., 2010. zTrap: zebrafish gene trap and enhancer trap database. *BMC developmental biology*, 10(1), p.105.
- Kawakami, K. & Shima, A., 1999. Identification of the Tol2 transposase of the medaka fish *Oryzias latipes* that catalyzes excision of a nonautonomous Tol2 element in zebrafish *Danio rerio*. *Gene*, 240(1), pp.239–44.
- Kotani, T. et al., 2006. Transposon-mediated gene trapping in zebrafish. *Methods (San Diego, Calif.)*, 39(3), pp.199–206.
- Kurazono, H. et al., 1992. Minimal essential domains specifying toxicity of the light chains of tetanus toxin and botulinum neurotoxin type A. *The Journal of biological chemistry*, 267(21), pp.14721–9.
- Lammers, J.H. et al., 1988. Hypothalamic substrates for brain stimulation-induced patterns of

- locomotion and escape jumps in the rat. *Brain research*, 449(1–2), pp.294–310.
- Lillesaar, C., 2011. The serotonergic system in fish. *Journal of Chemical Neuroanatomy*, 41(4), pp.294–308.
- McPherson, A.D. et al., 2016. Motor Behavior Mediated by Continuously Generated Dopaminergic Neurons in the Zebrafish Hypothalamus Recovers after Cell Ablation. *Current Biology*, 26(2), pp.263–269.
- Mueller, T. & Wullimann, M.F., 2015. *Atlas of early zebrafish brain development : a tool for molecular neurogenetics*,
- Mukamel, E.A., Nimmerjahn, A. & Schnitzer, M.J., 2009. Automated Analysis of Cellular Signals from Large-Scale Calcium Imaging Data. *Neuron*, 63(6), pp.747–760.
- Muto, A. et al., 2011. Genetic visualization with an improved GCaMP calcium indicator reveals spatiotemporal activation of the spinal motor neurons in zebrafish. *Proceedings of the National Academy of Sciences*, 108(13), pp.5425–5430.
- Muto, A. et al., 2013. Real-Time Visualization of Neuronal Activity during Perception. *Current Biology*, 23(4), pp.307–311.
- Muto, A. & Kawakami, K., 2016. Calcium Imaging of Neuronal Activity in Free-Swimming Larval Zebrafish. In *Methods in molecular biology*. pp. 333–341.
- Muto, A. & Kawakami, K., 2013. Prey capture in zebrafish larvae serves as a model to study cognitive functions. *Frontiers in Neural Circuits*, 7, p.110.
- Nakai, J., Ohkura, M. & Imoto, K., 2001. A high signal-to-noise Ca(2+) probe composed of a single green fluorescent protein. *Nature Biotechnology*, 19(2), pp.137–141.
- Pnevmatikakis, E.A. et al., 2016. Simultaneous Denoising, Deconvolution, and Demixing of Calcium Imaging Data. *Neuron*, 89(2), pp.285–299.

- Prober, D.A. et al., 2008. Zebrafish TRPA1 Channels Are Required for Chemosensation But Not for Thermosensation or Mechanosensory Hair Cell Function. *Journal of Neuroscience*, 28(40).
- Randlett, O. et al., 2015. Whole-brain activity mapping onto a zebrafish brain atlas. *Nature Methods*, 12(11), pp.1039–1046.
- Rink, E. & Guo, S., 2004. The too few mutant selectively affects subgroups of monoaminergic neurons in the zebrafish forebrain. *Neuroscience*, 127(1), pp.147–154.
- Rink, E. & Wullimann, M.F., 2001. The teleostean (zebrafish) dopaminergic system ascending to the subpallium (striatum) is located in the basal diencephalon (posterior tuberculum). *Brain research*, 889(1–2), pp.316–30.
- Schneider, C.A., Rasband, W.S. & Eliceiri, K.W., 2012. NIH Image to ImageJ: 25 years of image analysis. *Nature methods*, 9(7), pp.671–5.
- Semenova, S.A. et al., 2014. The tyrosine hydroxylase 2 (TH2) system in zebrafish brain and stress activation of hypothalamic cells. *Histochemistry and Cell Biology*, 142(6), pp.619–633.
- Severi, K.E. et al., 2014. Neural Control and Modulation of Swimming Speed in the Larval Zebrafish. *Neuron*, 83(3), pp.692–707.
- Shik, M.L., Severin, F. V & Orlovskii, G.N., 1966. [Control of walking and running by means of electric stimulation of the midbrain]. *Biofizika*, 11(4), pp.659–66.
- Sinnamon, H.M., 1993. Preoptic and hypothalamic neurons and the initiation of locomotion in the anesthetized rat. *Progress in neurobiology*, 41(3), pp.323–44.
- Sternberg, J.R. et al., 2016. Optimization of a Neurotoxin to Investigate the Contribution of Excitatory Interneurons to Speed Modulation In Vivo. *Current biology : CB*, 26(17),

pp.2319–28.

Umeda, K. et al., 2013. Targeted expression of a chimeric channelrhodopsin in zebrafish under regulation of Gal4-UAS system. *Neuroscience research*, 75(1), pp.69–75.

Urasaki, A., Morvan, G. & Kawakami, K., 2006. Functional Dissection of the Tol2 Transposable Element Identified the Minimal cis-Sequence and a Highly Repetitive Sequence in the Subterminal Region Essential for Transposition. *Genetics*, 174(2).

Yokogawa, T., Hannan, M.C. & Burgess, H.A., 2012. The Dorsal Raphe Modulates Sensory Responsiveness during Arousal in Zebrafish. *Journal of Neuroscience*, 32(43), pp.15205–15215.

Table 1. Transgenic Gal4 lines with expression in the hypothalamus of larval zebrafish

Line name	Brain expression pattern
gSA2AzGFF368A	Hypothalamus
gSAIzGFFD761A	Rostral hypothalamus
gSAIzGFFD946A	Hypothalamus
gSAIzGFFD1380A	Hypothalamus
gSAIzGFFM116A	Caudal hypothalamus, intermediate hypothalamus, paraventricular organ
gSAIzGFFM1013A	Caudal hypothalamus, intermediate hypothalamus, paraventricular organ
gSAIzGFFM1083A	Caudal hypothalamus, intermediate hypothalamus, paraventricular organ
gSAIzGFFM1121A	Caudal hypothalamus, intermediate hypothalamus, paraventricular organ, telencephalon
hspzGFFgDMC145F	Hypothalamus, preoptic area
SAGFF(LF)19C	Hypothalamus, forebrain
SAGFF(LF)67A	Hypothalamus, spinal cord
SAGFF(LF)120A	Hypothalamus, olfactory bulb
SAGFF(LF)178H	Hypothalamus, preoptic area
SAGFF(LF)224A	Hypothalamus, preoptic area
hspGFFDMC76A	Inferior lobe of hypothalamus, preoptic area

As examples, list showing 15 of the 54 transgenic zebrafish lines in which Gal4 expression (visualized using UAS:GFP effector fish) was found to be in the hypothalamus at 5 dpf larval stage. The line names and their respective GFP expression patterns in the brain of the zebrafish larvae are described. These lines were generated as part of an ongoing screen, using the *To12* mediated gene trap and enhancer trap methods. Individual Gal4 constructs have been described in the Materials and Methods section.

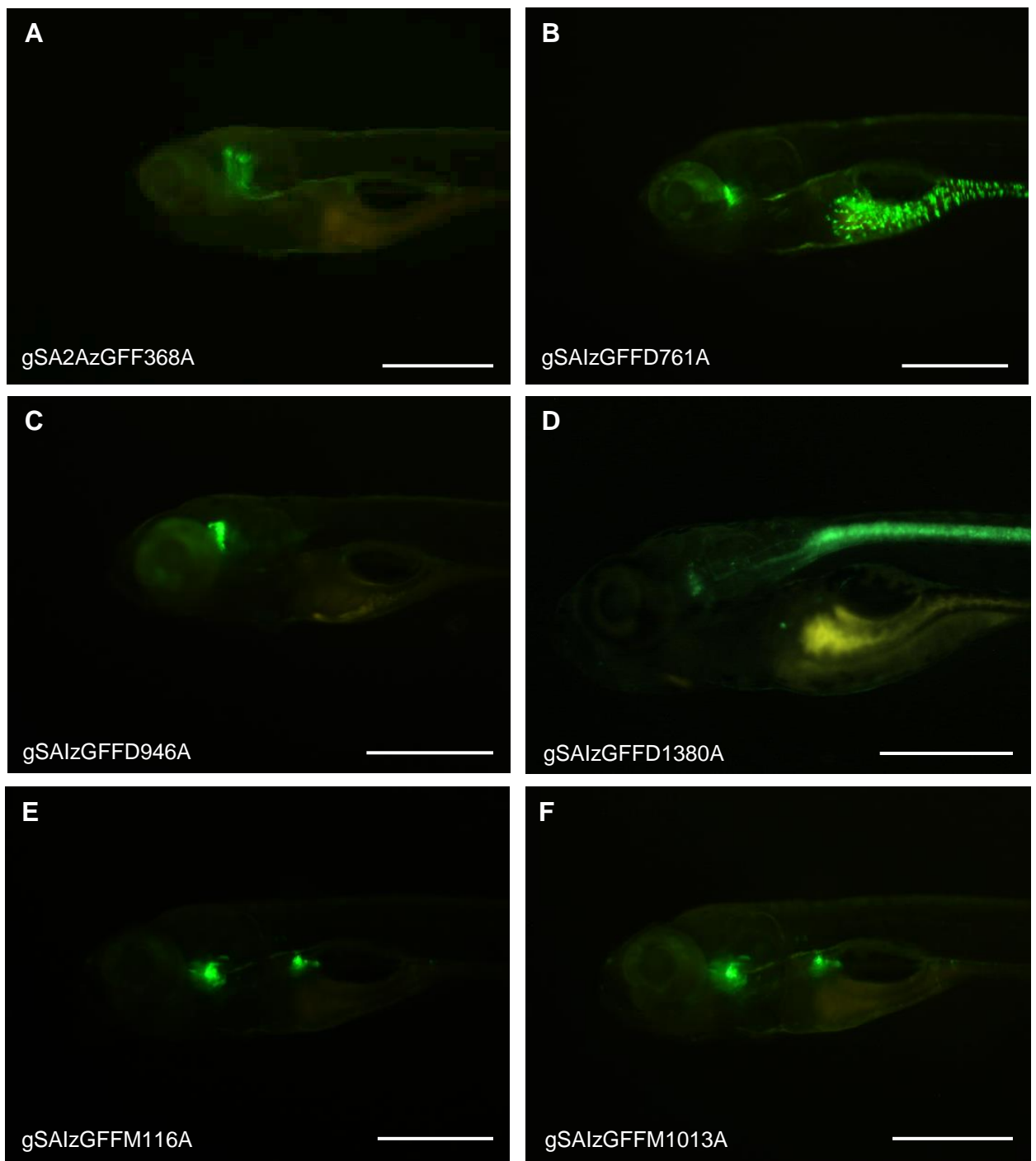


Figure 1. Transgenic Gal4 lines with expression in the hypothalamus of larval zebrafish

Gal4 expression patterns of the 15 lines listed in Table 1, visualized using the UAS:GFP effector fish. GFP fluorescence in the brain of double transgenic larvae at 5 dpf imaged from lateral side using a fluorescence stereomicroscope. Scale bars represent 500 μm.

A: gSA2AzGFF368A; UAS:GFP

B: gSAIzGFFD761A; UAS:GFP

C: gSAIzGFFD946A; UAS:GFP

D: gSAIzGFFD1380A; UAS:GFP

E: gSAIzGFFM116A; UAS:GFP

F: gSAIzGFFM1013A; UAS:GFP

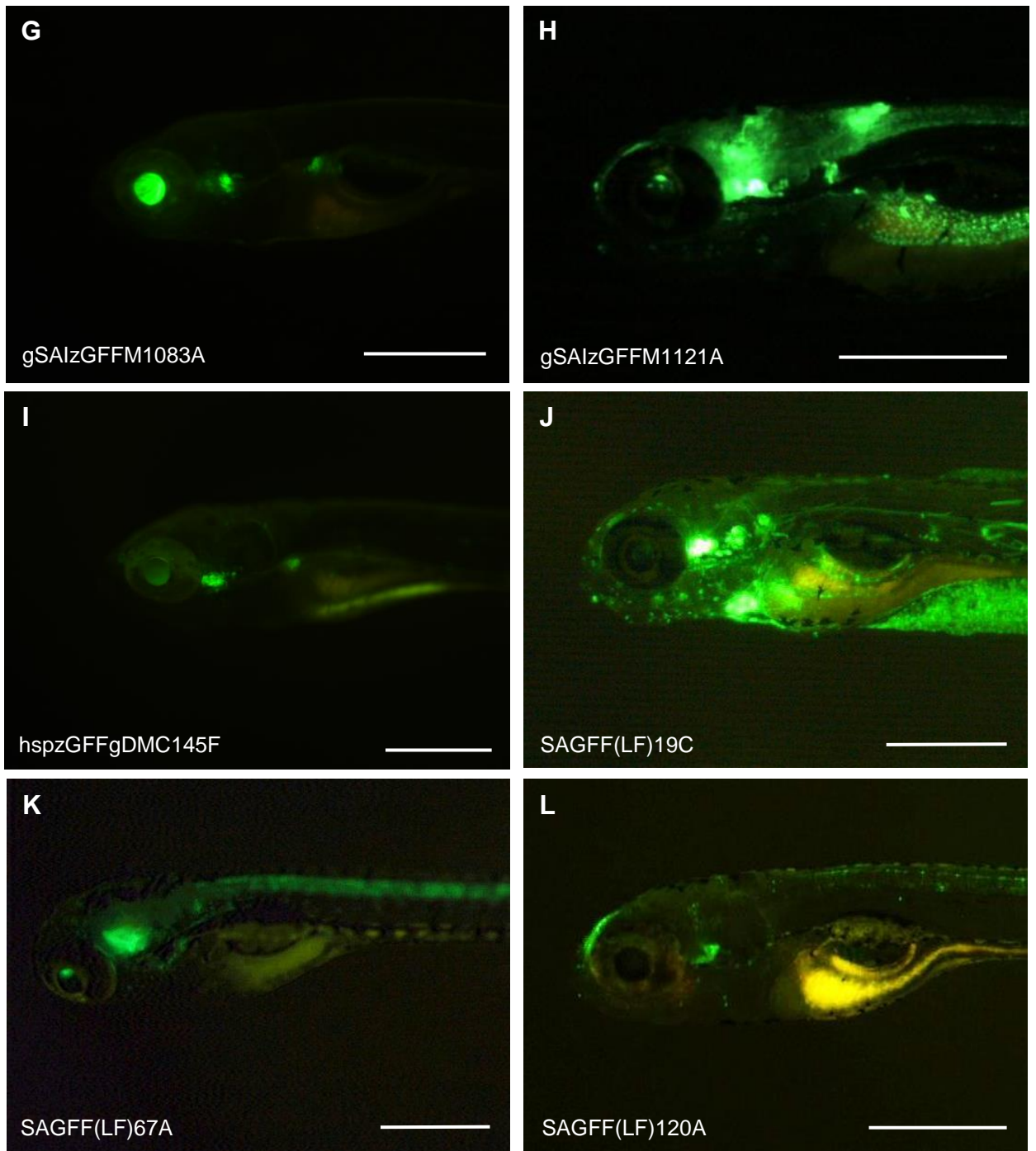


Figure 1. Continued

G: gSAIzGFFM1083A; UAS:GFP

H: gSAIzGFFM1121A; UAS:GFP

I: hspzGFFgDMC145F; UAS:GFP

J: SAGFF(LF)19C; UAS:GFP

K: SAGFF(LF)67A; UAS:GFP

L: SAGFF(LF)120A; UAS:GFP

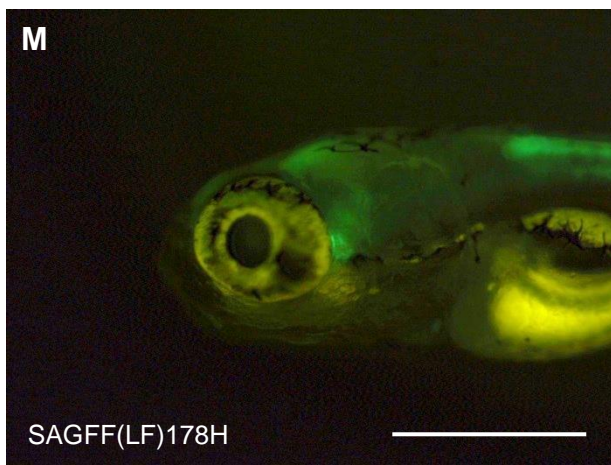


Figure 1. Continued

M: SAGFF(LF)178H; UAS:GFP

N: SAGFF(LF)224A; UAS:GFP

O: hspGFFgDMC76A; UAS:GFP

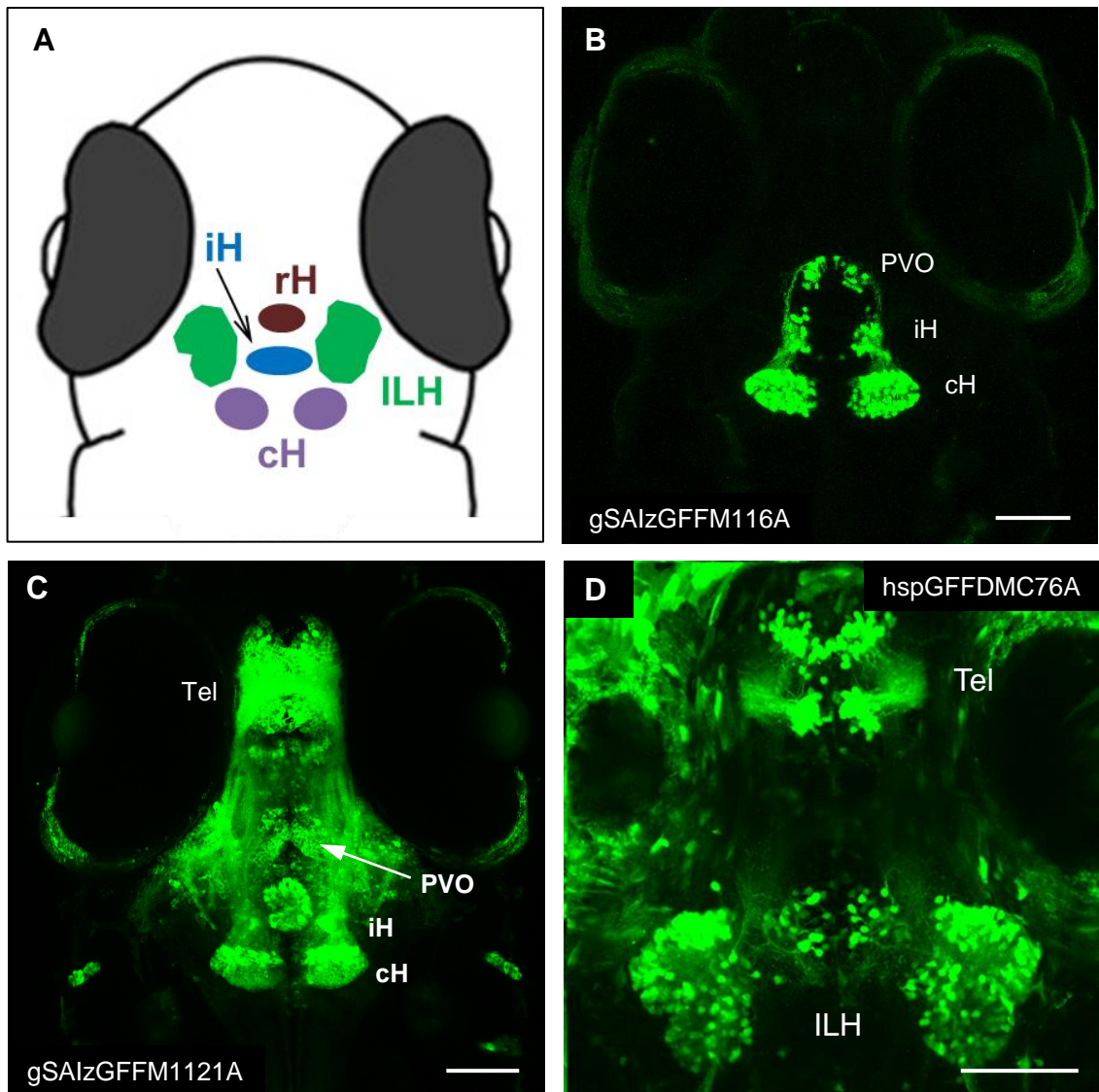


Figure 2. Transgenic Gal4 lines labeling specific hypothalamic nuclei in larval zebrafish

A: Schematic showing various hypothalamus nuclei defined in zebrafish brain atlas (Mueller & Wullimann 2015) in the larval zebrafish brain, namely the rostral hypothalamus (rH), the intermediate hypothalamus (iH), the caudal hypothalamus (cH), and the inferior lobe of the hypothalamus (ILH).

B-D: GFP fluorescence in the brain of double transgenic larvae at 5 dpf, visualized from dorsal side using a two-photon microscope. **B,** gSAIzGFFM116A; UAS:GFP larvae express GFP in a neuronal population in the cH, iH, and PVO. **C,** gSAIzGFFM1121A; UAS:GFP larvae express GFP in a neuronal population in the cH, iH, PVO and the telencephalon. **D,** hspGFFDMC76A; UAS:GFP larvae express GFP in a subpopulation in the ILH and the telencephalon.

cH: caudal hypothalamus, iH: intermediate hypothalamus, ILH: inferior lobe of hypothalamus, PVO: paraventricular organ, Tel: telencephalon

Scale bars represent 75 μ m

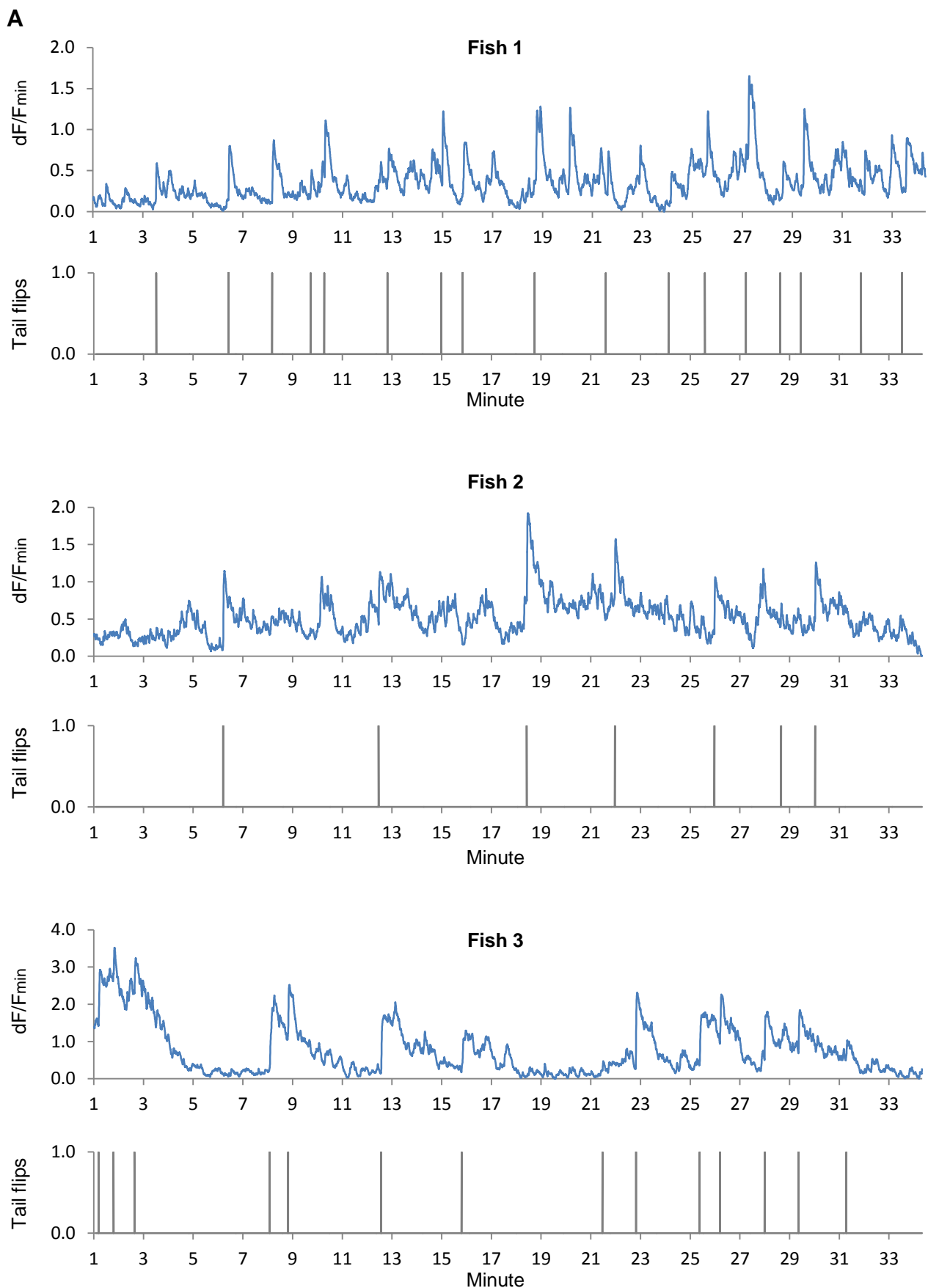


Figure 3. Neuronal populations labeled by the 116A-gal4 and 1121A-gal4 lines are activated when fish perform tail-flips

A: Graphs showing normalized GCaMP6s fluorescence intensities (dF/F_{min}) in the 116A-neurons in three 116A-gal4; UAS:GCaMP6s larvae during spontaneous tail-flips. Tail-flips were detected by calculating the mean intensities from ROIs on tails. A change in mean intensity of more than 1 standard deviation between consecutive frames was scored as a tail-flip. Recording of GCaMP6s fluorescence and tail position was done at 5 fps.

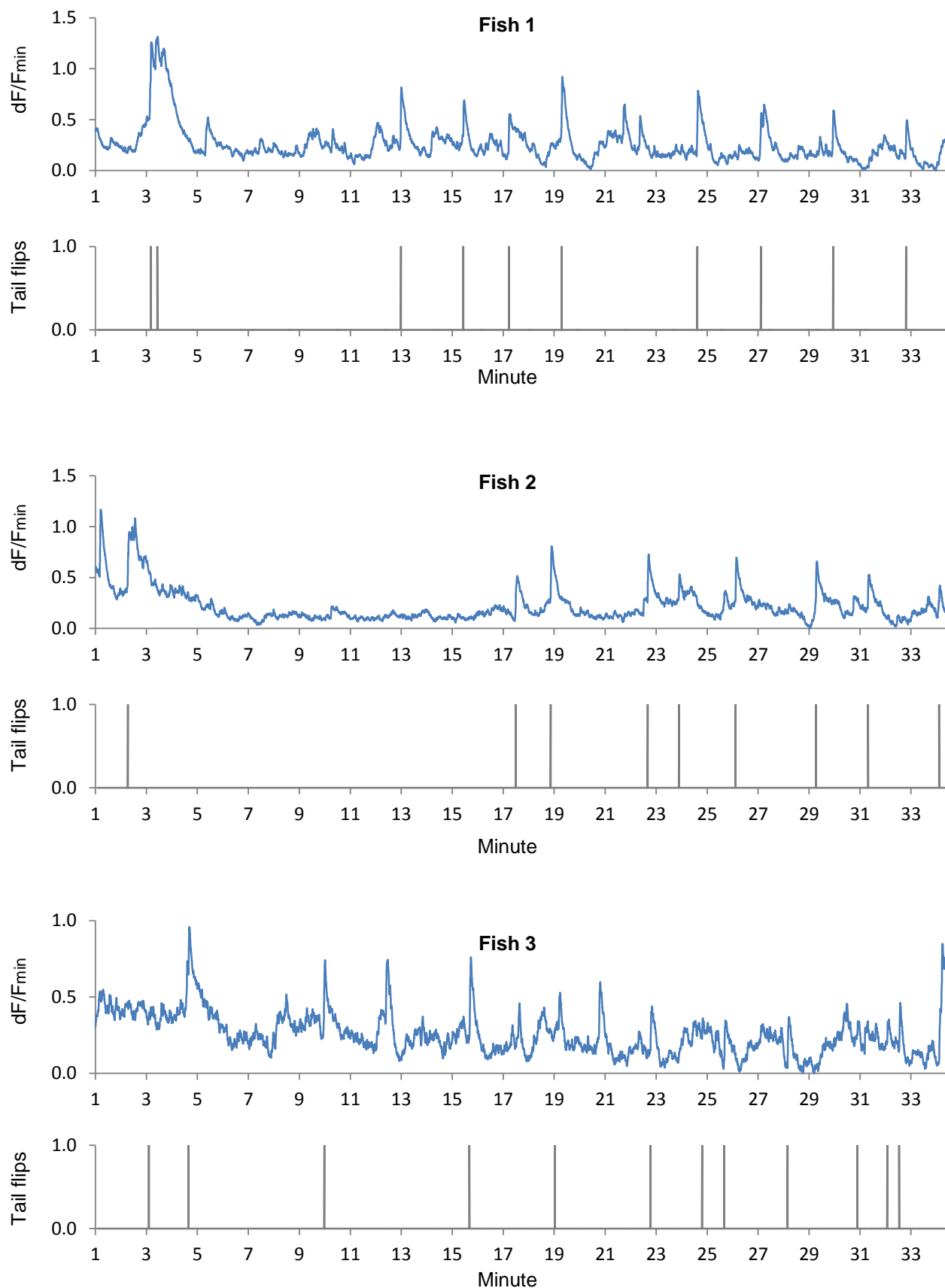
B

Figure 3. Neuronal populations labeled by the 116A-gal4 and 1121A-gal4 lines are activated when fish perform tail-flips

B: Graphs showing normalized GCaMP6s fluorescence intensities (dF/Fmin) in the 1121A-neurons in cH, iH and PVO (dF/Fmin) in three 1121A-gal4; UAS:GCaMP6s larvae during spontaneous tail-flips. Tail-flips were detected by calculating the mean intensities from ROIs on tails. A change in mean intensity of more than 1 standard deviation between consecutive frames was scored as a tail-flip. Recording of GCaMP6s fluorescence and tail position was done at 5 fps.

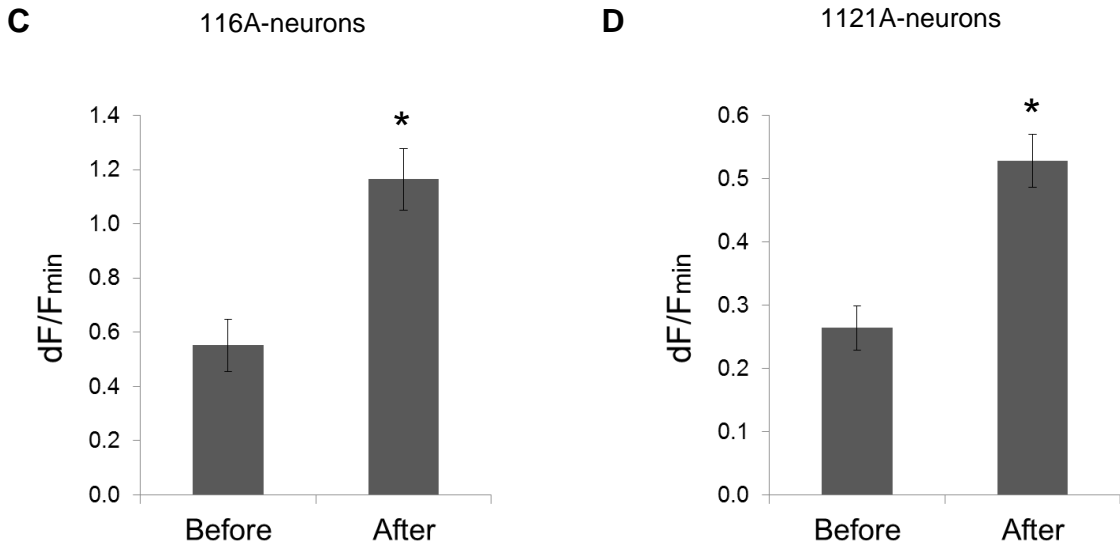


Figure 3. Neuronal populations labeled by the 116A-gal4 and 1121A-gal4 lines are activated when fish perform tail-flips

C-D: Graphs comparing average spontaneous neural activities during 10 seconds before initiation of tail flips with the average neural activities during 10 seconds after initiation of tail-flips in head-restrained larvae. Neuronal populations labeled by 116A-gal4 (**C**) and 1121A-gal4 (in cH, iH and PVO) (**D**) lines showed significantly higher average activity during 10 seconds after initiation of tail-flips.

116A-gal4; UAS:GCaMP6s, n = 3 fish, 38 tail-flips.

1121A-gal4; UAS:GCaMP6s, n = 3 fish, 31 tail-flips.

Asterisk indicates two-tailed $P < 10^{-4}$, paired *t* test. Error bars = SEM.

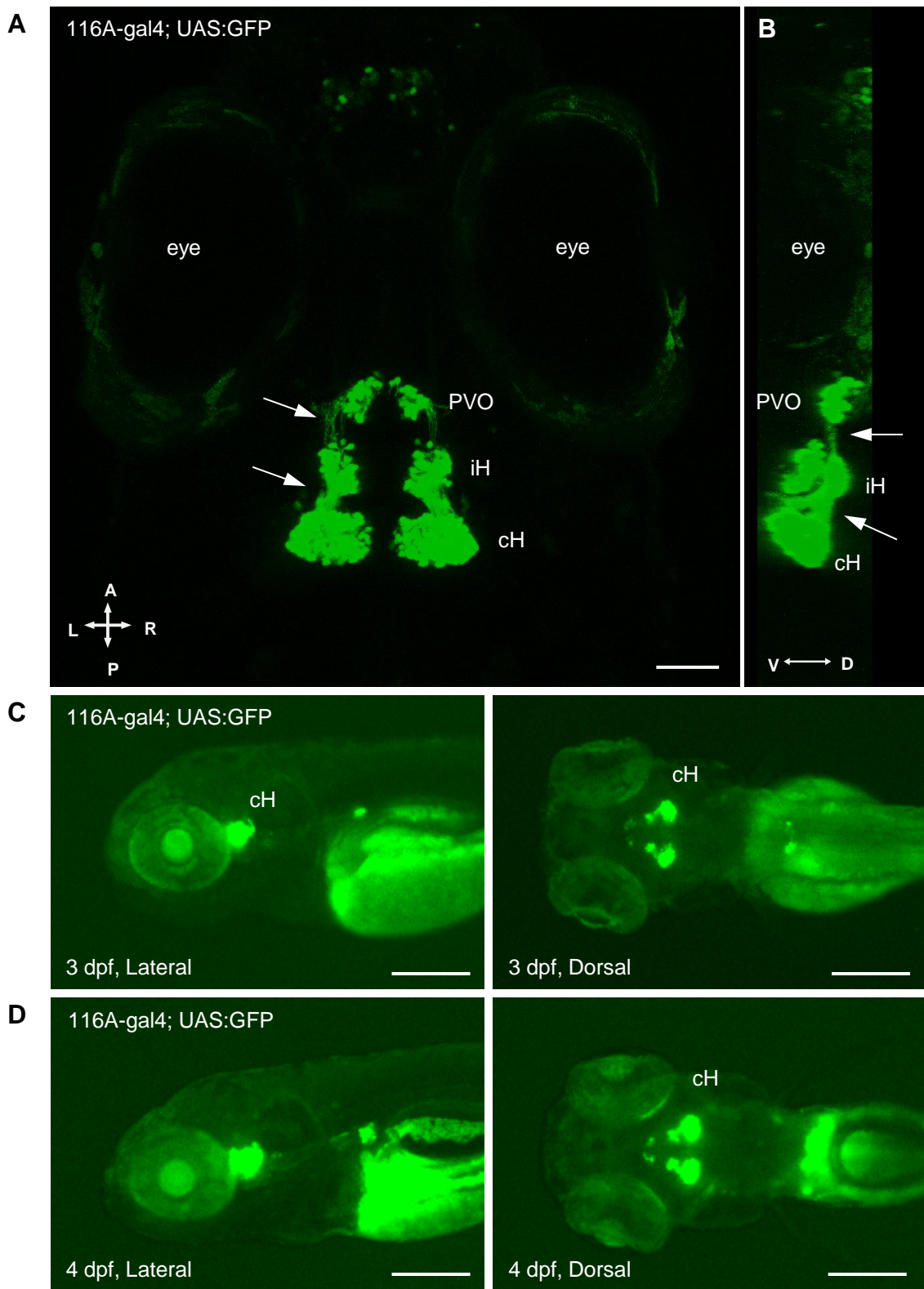


Figure 4. GFP expression pattern in 116A-gal4; UAS:GFP fish at larval stage

A-B: Dorsal (**A**) and lateral (**B**) views of 116A-gal4; UAS:GFP larvae at 5 dpf, analyzed using two-photon microscope. GFP is expressed in a neuronal population in the cH, iH, and PVO. Arrows indicate GFP-labeled projections between cells in the cH, iH and PVO. Scale bar (same for A and B) represents 50 μ m.

C-D: Lateral and dorsal views of 116A-gal4; UAS:GFP larvae at 3 dpf (**C**) and 4 dpf (**D**). GFP expression in the cH, iH and PVO is visible at 3 dpf. Scale bars represent 200 μ m.

cH: caudal hypothalamus, iH: intermediate hypothalamus, PVO: paraventricular organ.

L: left, R: right, A: anterior, P: posterior, V: ventral, D: dorsal

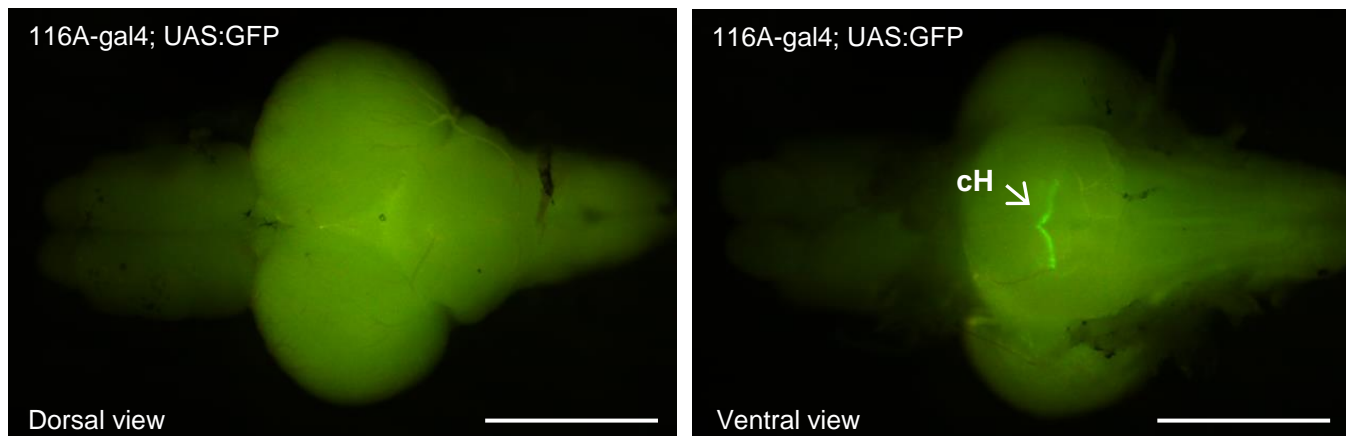
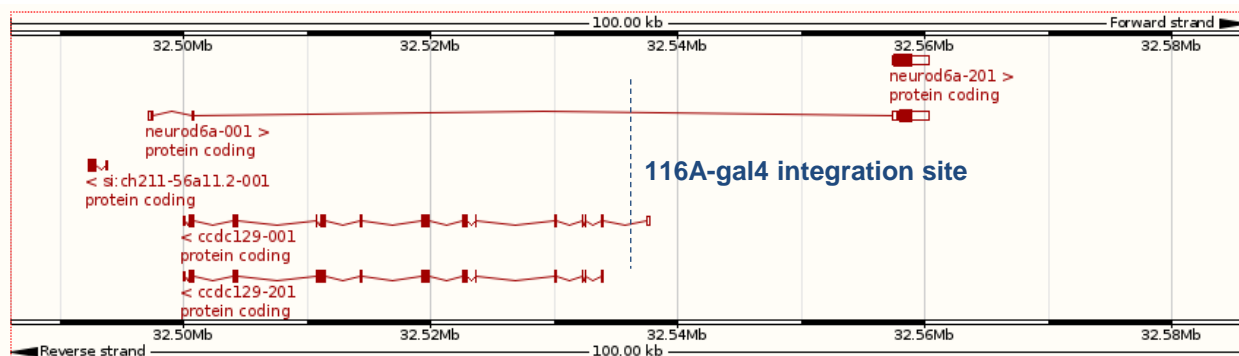
A**B**

Figure 5. GFP expression in 116A-gal4; UAS:GFP fish at adult stage

A: Dorsal and ventral views of brain of adult 116A-gal4; UAS:GFP fish, analyzed using fluorescence stereomicroscope. GFP expression is visible in the cH in the ventral view of the adult brain. Scale bars represent 1 mm.

B: Gal4 integration site of 116A-gal4 line is located in Ensembl Zv10 zebrafish genome database. Gal4 transposon is integrated at position 33656046 on chromosome 24 in the intronic sequences of two overlapping genes, *neurod6a* and *ccdc129*.

cH: caudal hypothalamus

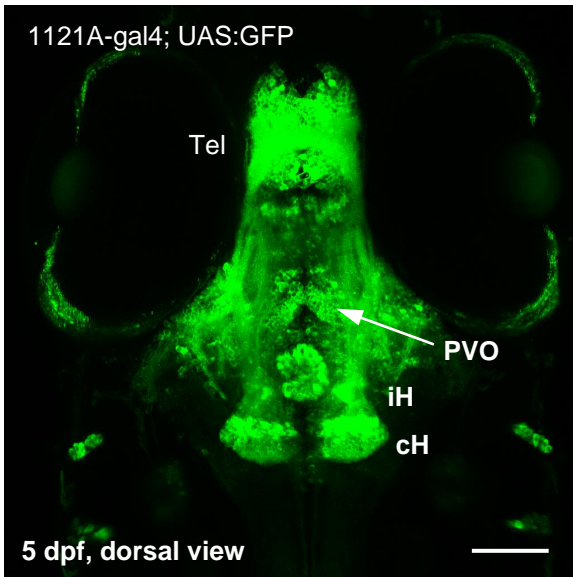
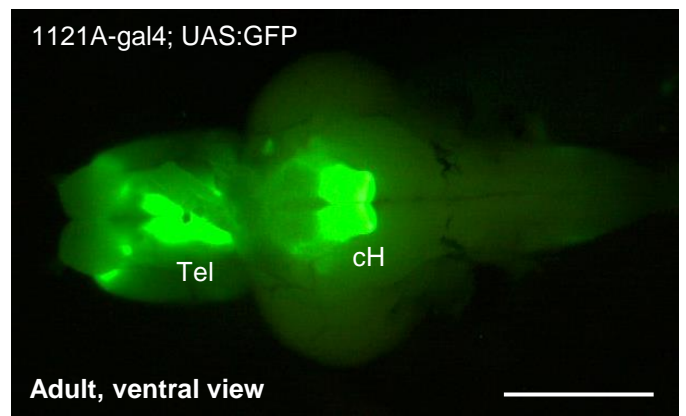
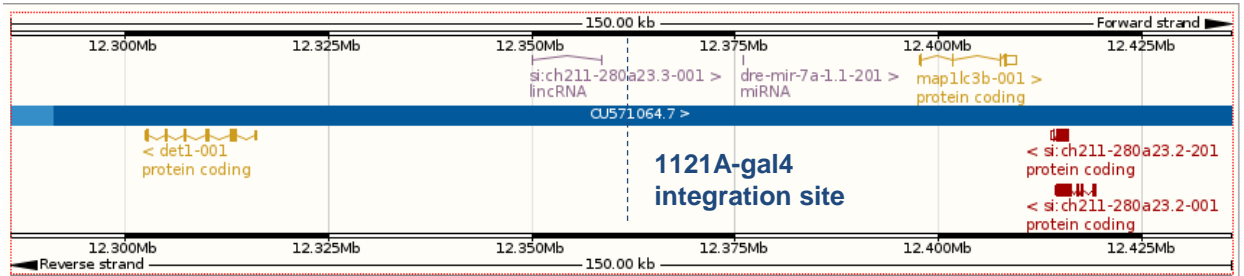
A**B****C**

Figure 6. GFP expression in 1121A-gal4; UAS:GFP fish at larval and adult stages

A: GFP expression pattern in 1121A-gal4; UAS:GFP fish larvae at 5 dpf, visualized using two-photon microscope. Scale bar represents 75 μ m.

B: GFP expression pattern in 1121A; UAS:GFP fish at adult stage. Scale bar represents 1 mm.

C: Gal4 integration site of 1121A-gal4 line is located in Ensembl Zv10 zebrafish genome database. Gal4 transposon is integrated at position 13589499 on chromosome 25 in an intergenic region.

cH: caudal hypothalamus, iH: intermediate hypothalamus, PVO: paraventricular organ, Tel: telencephalon

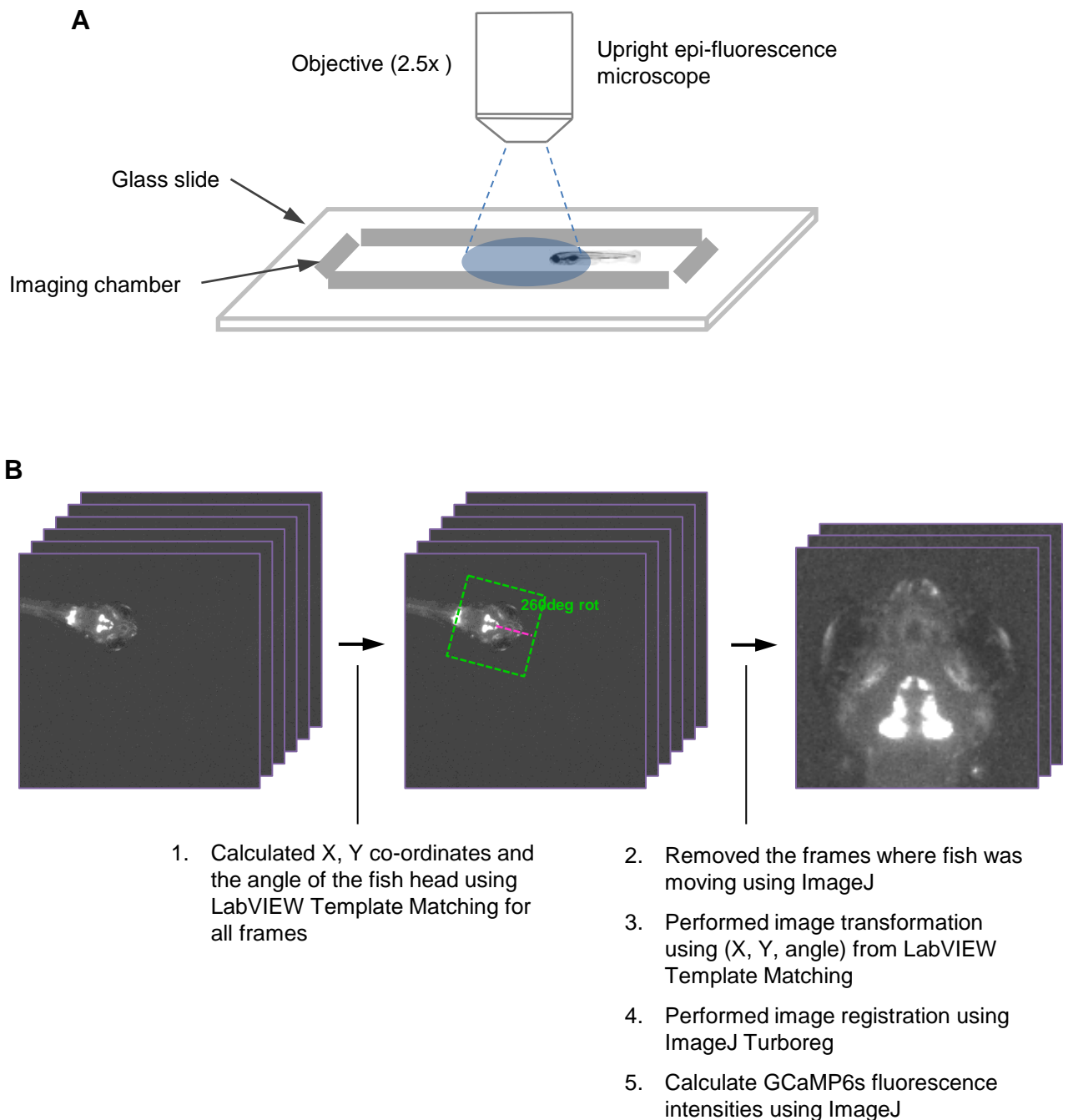


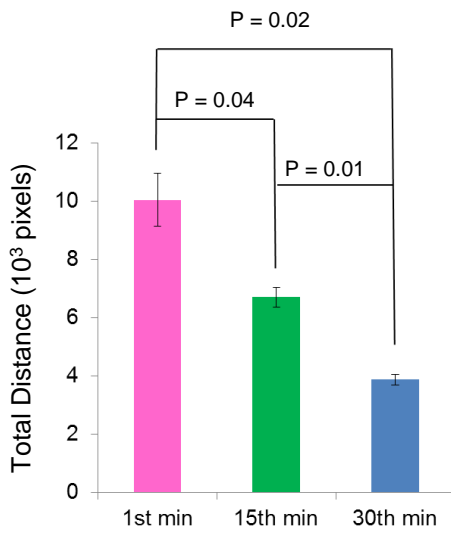
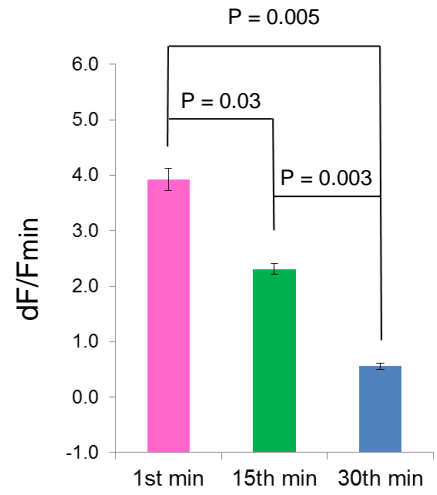
Figure 7. Functional imaging of the 116A-neurons in freely swimming zebrafish

A, Experimental system for functional calcium imaging in freely swimming larvae.

116A-gal4; UAS:GCaMP6s larvae were placed in a rectangular imaging chamber made on a glass slide. GCaMP6s fluorescence in the freely swimming larvae was recorded using an upright epi-fluorescence microscope during 30 minutes of habituation in the imaging chamber.

B, Analysis of GCaMP6s fluorescence intensity in freely swimming 116A-gal4; UAS:GCaMP6s larvae.

X, Y co-ordinates and the angle of the fish head were calculated using LabVIEW Template Matching for all frames. The frames in which fish was moving or missing were removed using ImageJ. Image transformation was performed using the (X, Y, angle) information. Finally, image registration was performed and GCaMP6s fluorescence intensities in the 116A-neurons were calculated using ImageJ.

A**B****Figure 8. Locomotor activities and activity of the 116A-neurons in freely swimming fish**

A-B: Graphs show average locomotor activity (total traveled distance) (**A**) and average normalized GCaMP6s fluorescence intensity (dF/Fmin) in 116A-neurons (**B**) of freely swimming 116A-gal4; UAS:GCaMP6s larvae, during the 1st, the 15th and the 30th minute of habituation in the imaging chamber. $n = 3$ fish, the two-tailed P values from paired t test are indicated in the graphs. Error bars represent SEM.

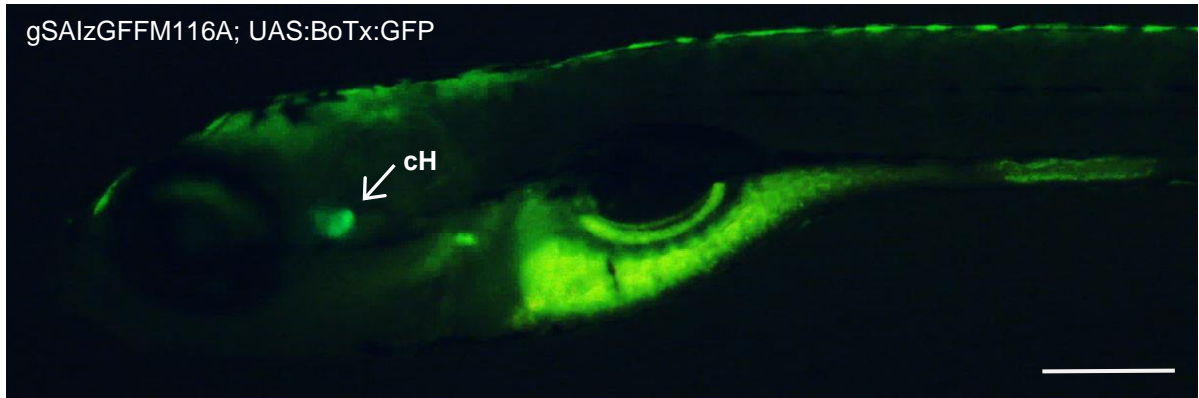


Figure 9. Expression of BoTx:GFP transgene in 116A-gal4; UAS:BoTx:GFP larvae

Lateral view of a 116A-gal4;UAS:BoTx:GFP larva at 5 dpf, showing the tagged-GFP expression from BoTx:GFP transgene in the 116A neurons in the cH. Fluorescence from the tagged-GFP was visualized using a fluorescence stereomicroscope. Scale bar represent 200 μ m.

cH: caudal hypothalamus

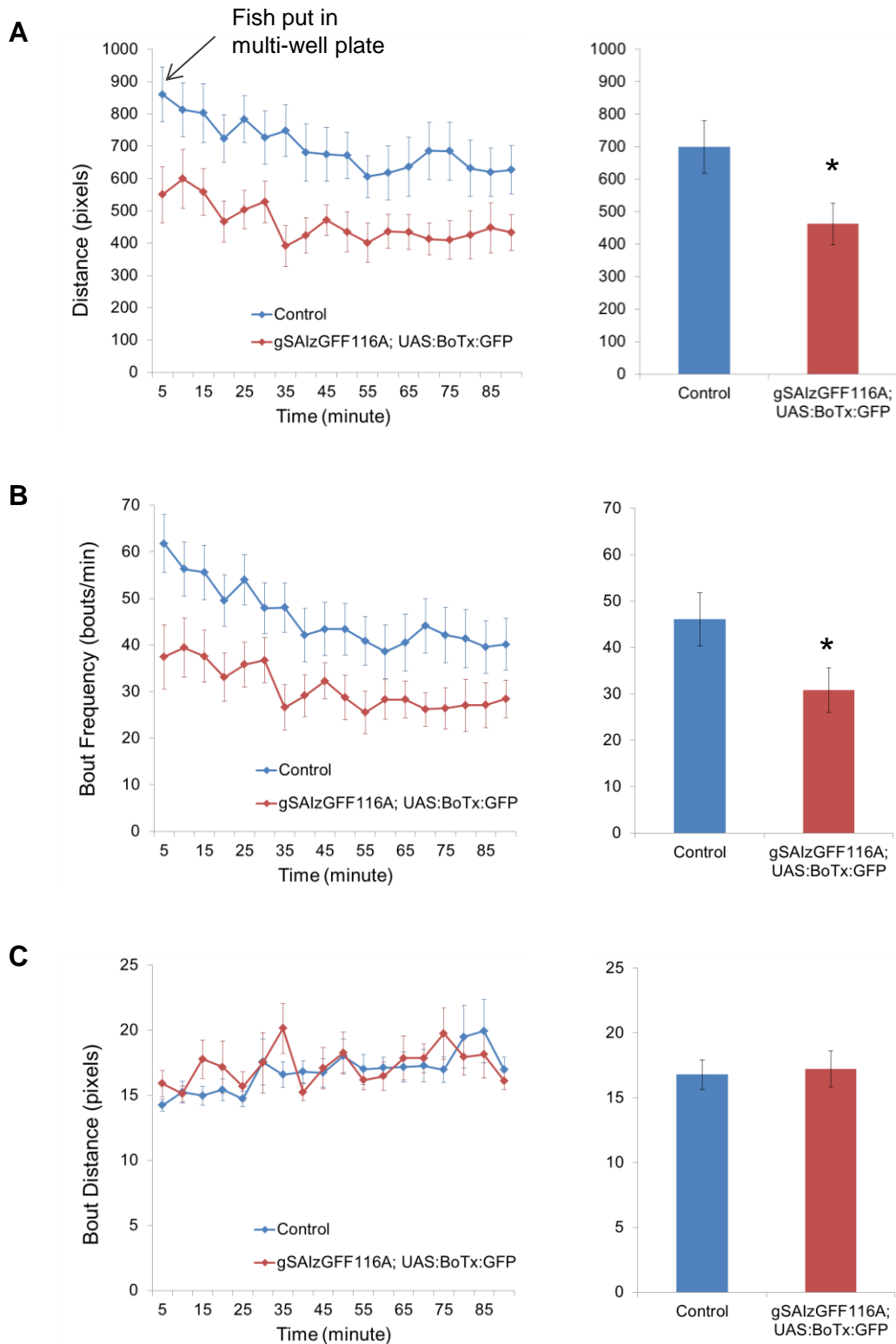


Figure 10. Effect of inhibition of the 116A-neurons on locomotor activity

A-C: Line graphs show locomotor activity (**A**), bout frequency (**B**) and average bout distance (**C**) of 116A-gal4; UAS:BoTx:GFP larvae and their control siblings after transfer to a multi-well plate. Bar graph shows same values averaged over time intervals. Asterisks represent significant reduction in 116A-gal4; UAS:BoTx:GFP group (n= 24 for each group, * P < 0.05, unpaired *t* test). Error bars represent SEM.

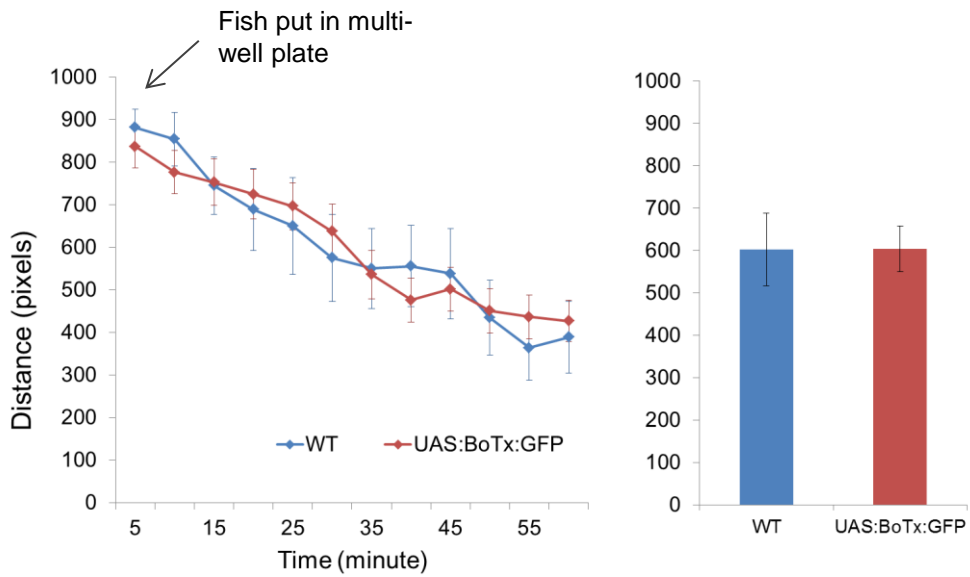


Figure 11. Effect of UAS:BoTx:GFP transgene alone on locomotor activity

Line graph shows locomotor activity of larvae carrying UAS:BoTx:GFP transgene alone after transfer to multi-well plate. Locomotor activity was calculated as average distance traveled per 5 minutes for 60 minutes. Bar graph shows same values averaged over 60 minutes intervals ($n = 12$ for WT, $n = 18$ for UAS:BoTx:GFP, $P = 0.98$, unpaired t test). Error bars represent SEM.

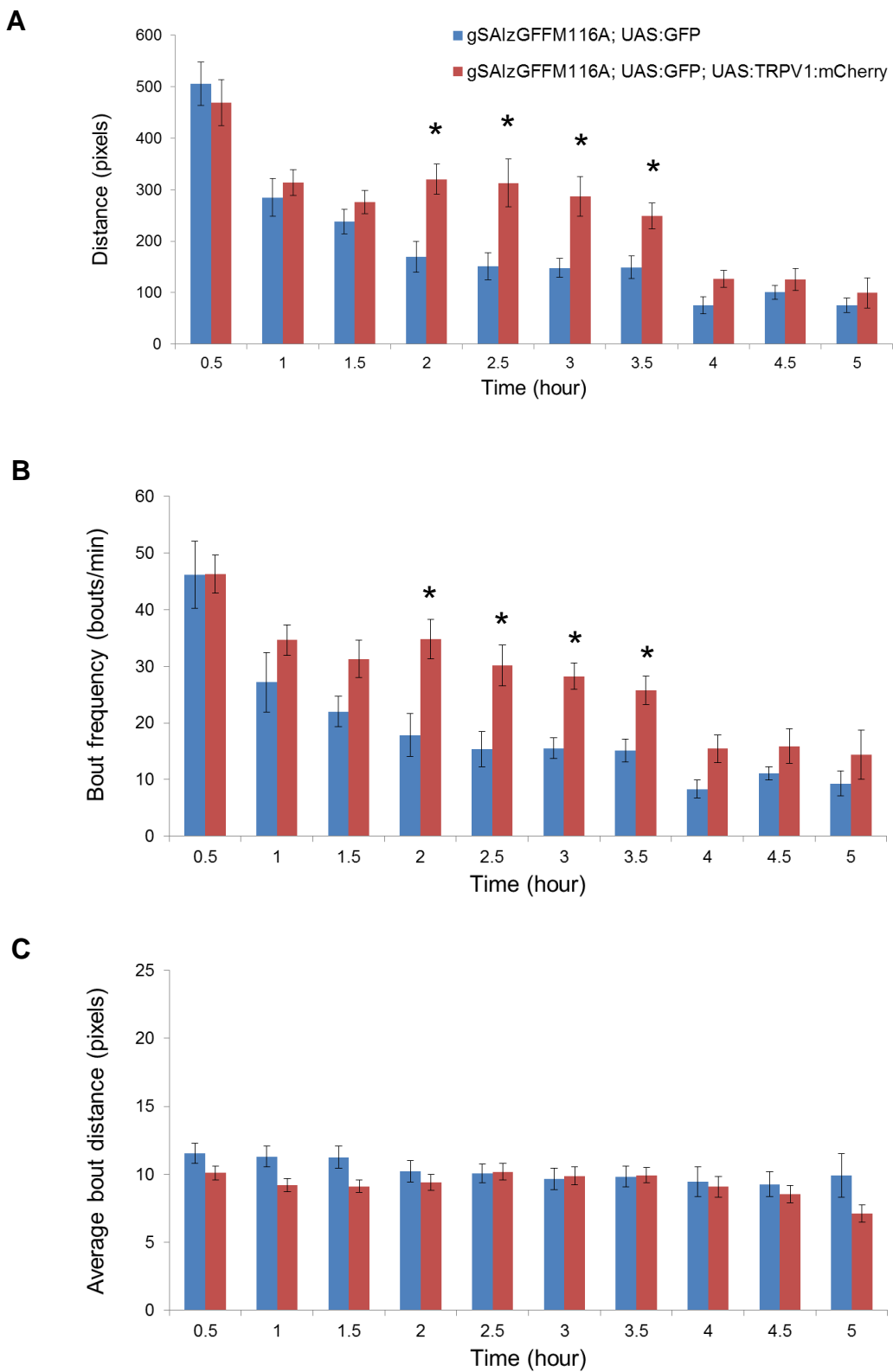


Figure 12. Effect of activation of the 116A-neurons on locomotor activity

A-C: Bar graphs show locomotor activity (**A**), bout frequency (**B**) and average bout distance (**C**) of 116A-gal4; UAS:TRPV1 larvae and their control siblings after transfer to a multi-well plate. Asterisks indicate significant difference in the swim parameters ($n = 8$ for 116A-gal4; UAS:GFP, $n = 13$ for 116A-gal4; UAS:GFP; UAS:TRPV1, * $P < 0.05$, unpaired t test). Error bars represent SEM.

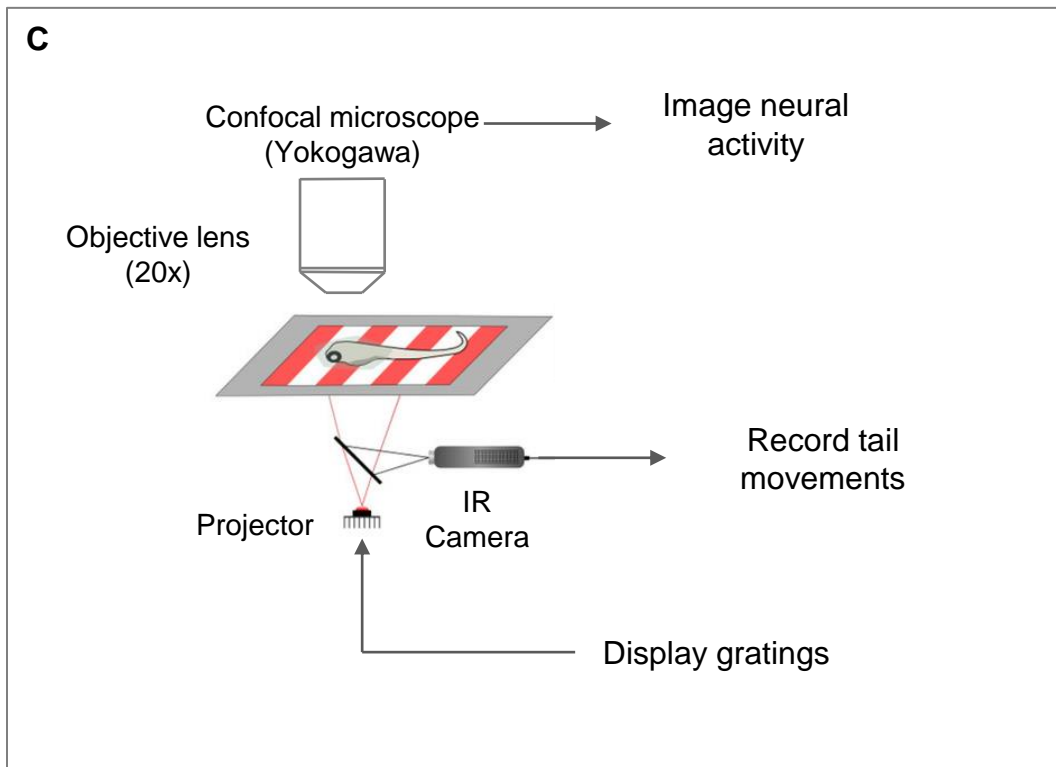
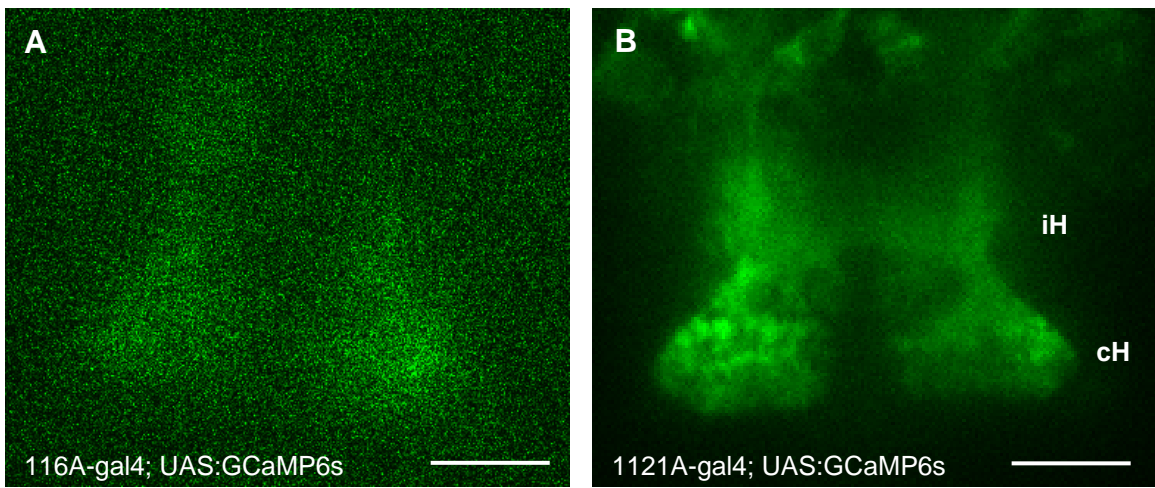


Figure 13. Functional imaging of the 1121A-neurons at single-cell resolution

A-B: GCaMP6s expression in a 116A-gal4; UAS:GCaMP6s (**A**) and 1121A-gal4; UAS:GCaMP6s (**B**) larva at 5 dpf, visualized using a spinning disk confocal microscope. Scale bars represent 50 μ m.

C: Experimental system to record neural activity from larval zebrafish brain during optomotor response.

cH: caudal hypothalamus, iH: intermediate hypothalamus

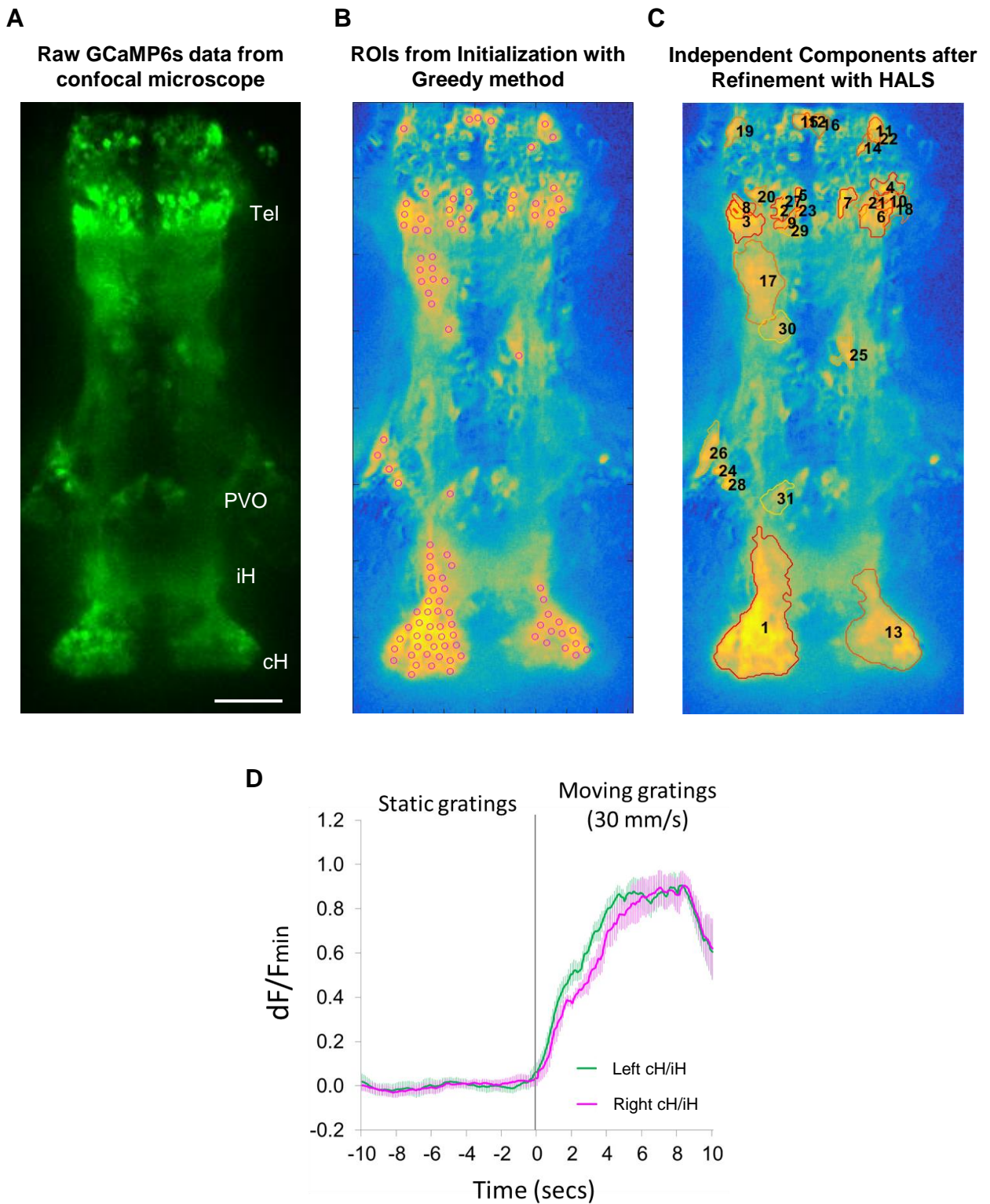


Figure 14. Activities of the hypothalamic 1121A-neurons during OMR

A: Raw GCaMP6s fluorescence intensity image from confocal microscope in 1121A-gal4; UAS:GCaMP6s larva during experiment. Scale bar represents 50 μm .

B: ROIs denoting individual neurons identified by initialization with Greedy method.

C: Independent components identified after grouping of spatial components and refinement with HALS.

D: Normalized GCaMP6s fluorescence intensity (dF/Fmin) in the 1121A-neurons in the left and the right cH/iH during 10 seconds before and after onset of OMR stimulus are shown. Activities of 1121A-neurons in the cH and the iH were synchronous, and increased upon onset of the moving gratings

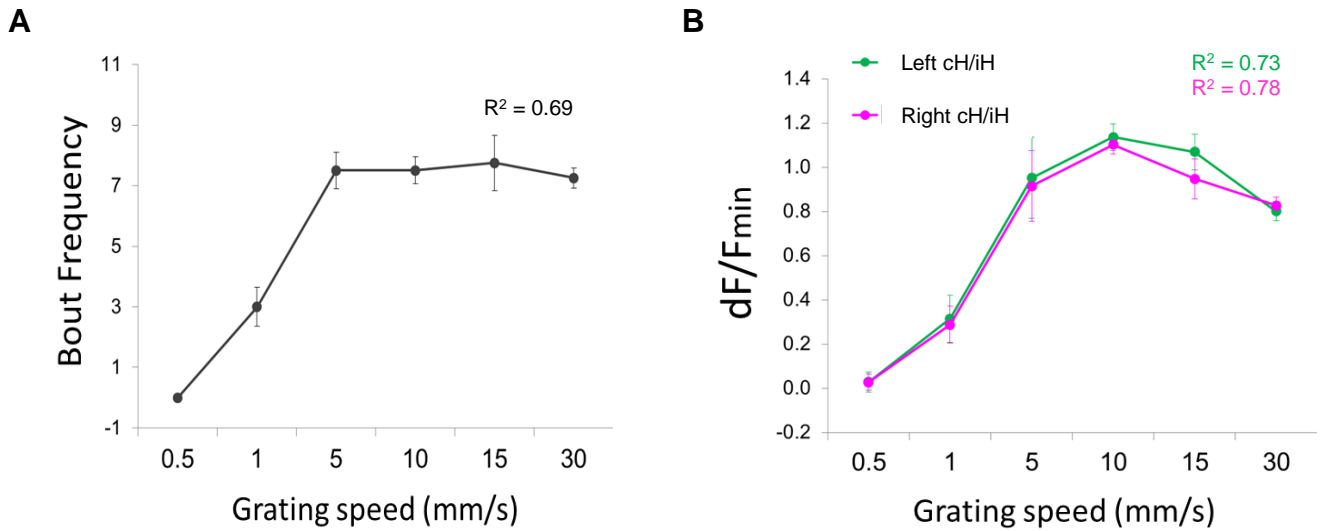


Figure 15. Tuning of activity of hypothalamic 1121A-neurons to the speed of OMR stimulus

A: Bout frequency of 1121A-gal4; UAS:GCaMP6s head restrained larvae for varying grating speeds. Average number of bouts during 10 seconds after onset of OMR stimulus are shown. $R^2 = 0.69$.

B: Normalized GCaMP6s fluorescence intensity (dF/Fmin) in 1121A-neurons in cH and iH during 10 seconds after onset of OMR stimulus. $R^2 = 0.73$ (left hemisphere), $R^2 = 0.78$ (right hemisphere).

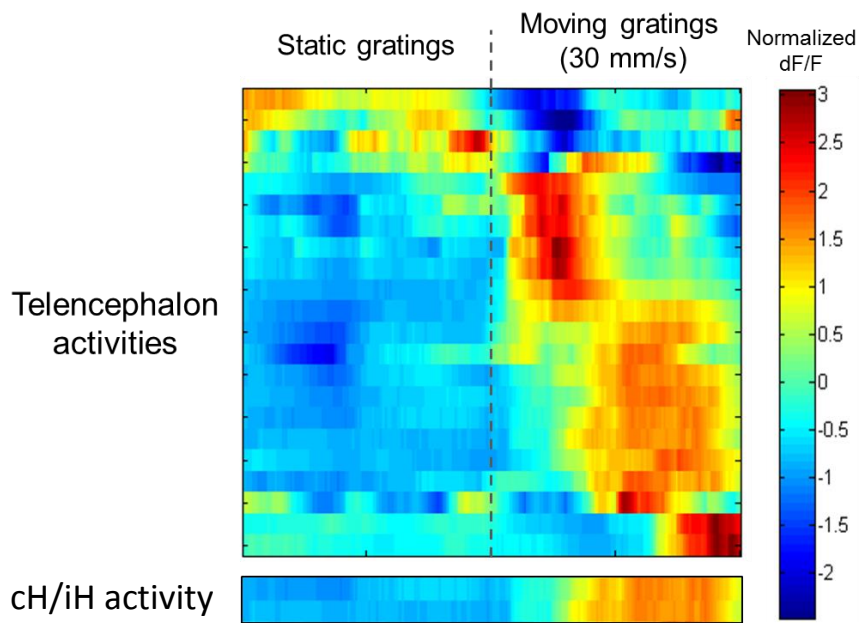


Figure 16. Activities of 1121A telencephalic neurons during OMR

Cluster analysis using pairwise correlations was performed to group telencephalic 1121A-neurons displaying similar activities during OMR. Several telencephalic 1121A-neurons were activated upon onset of moving gratings. Activities of some of the telencephalic 1121A-neurons were correlated with the activities of the 1121A-neurons in the cH/iH (bottom pane).

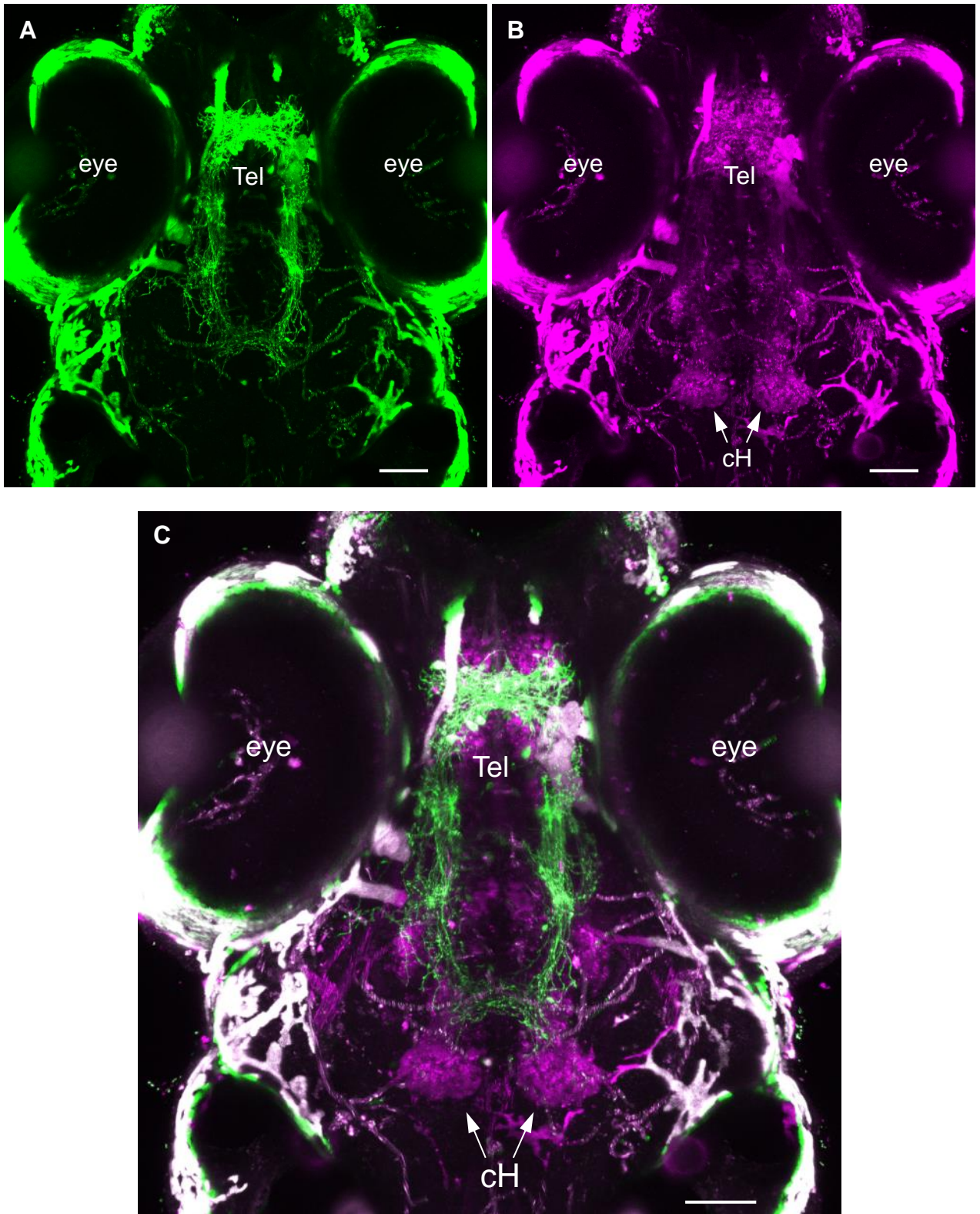


Figure 17. Projections of telencephalon neurons in 1121A-gal4; UAS:ChRWR:GFP; UAS:RFP fish
A-C: Expression pattern of ChRWR:GFP (A), RFP (B), and merged (C) were visualized in 1121A-gal4; UAS:ChRWR:GFP; UAS:RFP larvae at 5 dpf using two-photon microscope. Projections from telencephalon extending towards the hypothalamus were visible. Scale bars represent 50 μ m.

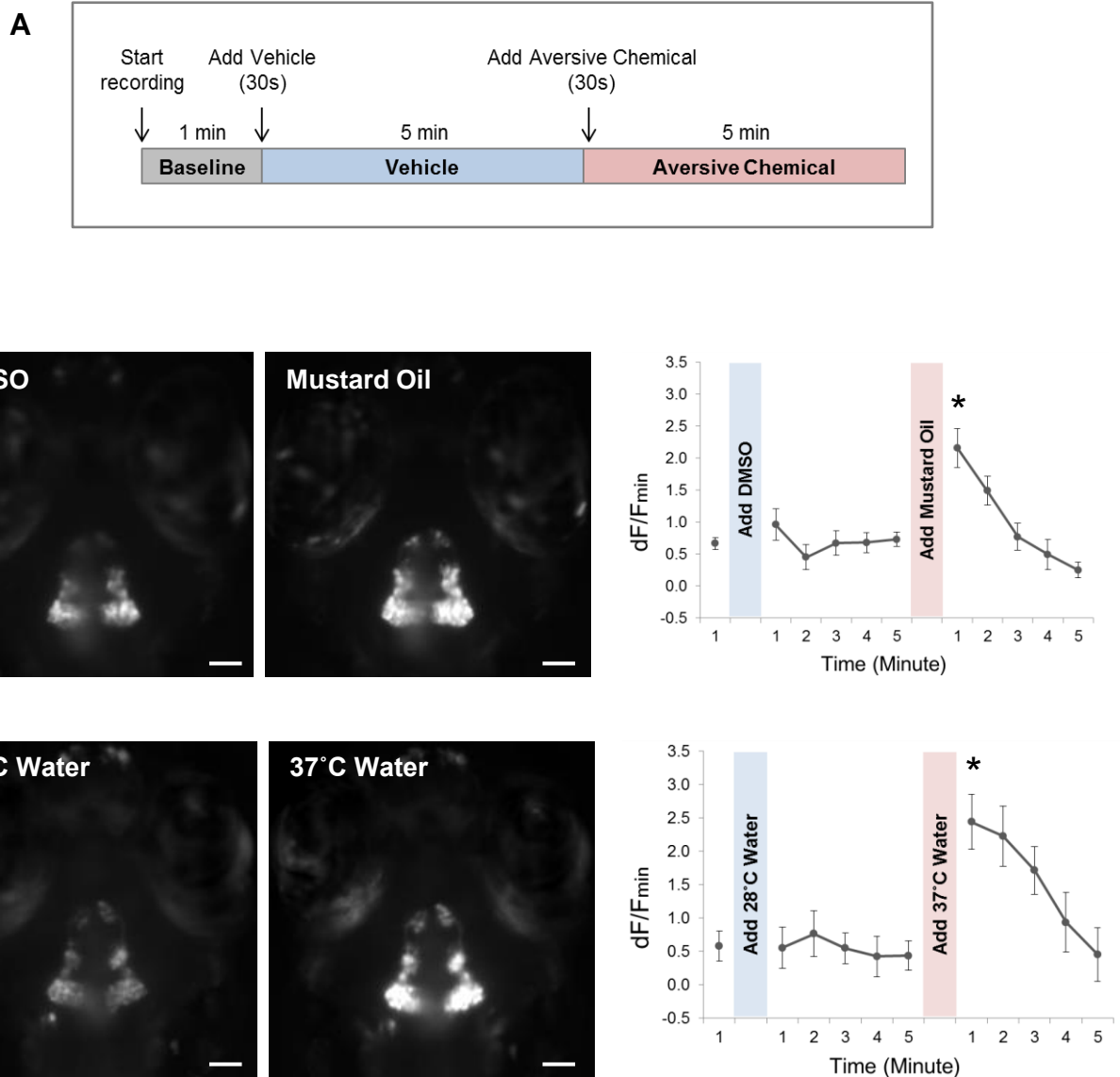


Figure 18. Activities of the 116A-neurons in response to aversive stimuli

A: Experimental protocol.

B-C: Activity of 116A-neurons in the cH in response to mustard oil (**B**) and hot water (**C**) in 5 dpf 116A-gal4; UAS:GCaMP6s larvae embedded in agarose. Images show the average GCaMP6s fluorescence intensity during first minute after addition of vehicle/aversive stimulus. Graphs show the average normalized GCaMP6s fluorescence intensity (dF/Fmin) in the 116A-neurons in the cH.

B: The activity of 116A-neurons in the cH during 1 minute after addition of DMSO (vehicle) was not significantly different than activity during 1 minute before adding DMSO ($n = 3$, $P = 0.29$, paired t test). The activity of 116A-neurons in the cH during 1 minute after addition of mustard oil was significantly higher than activity during 1 minute before adding mustard oil ($n = 3$, $*P = 0.02$, paired t test).

C: The activity of 116A-neurons in the cH during 1 minute after addition of 28°C water (control) was not significantly different than activity during 1 minute before adding 28°C water ($n = 3$, $P = 0.79$, paired t test). The activity of 116A-neurons in the cH during 1 minute after addition of 37°C water I was significantly higher than activity during 1 minute before adding 37°C water ($n = 3$, $*P = 0.01$, paired t test).

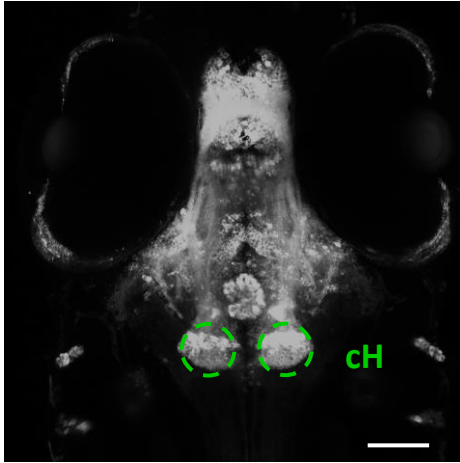
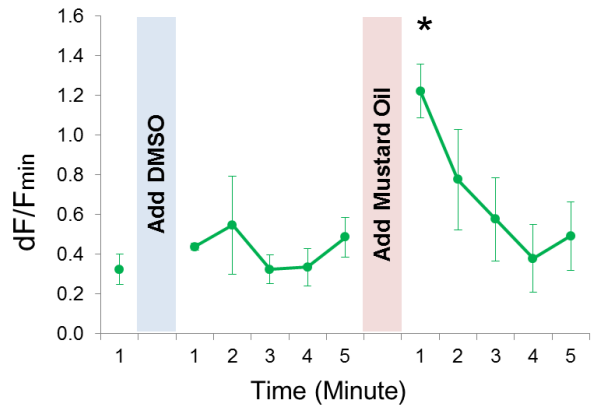
A**B**

Figure 19. Activities of the 1121A-neurons in response to aversive stimuli

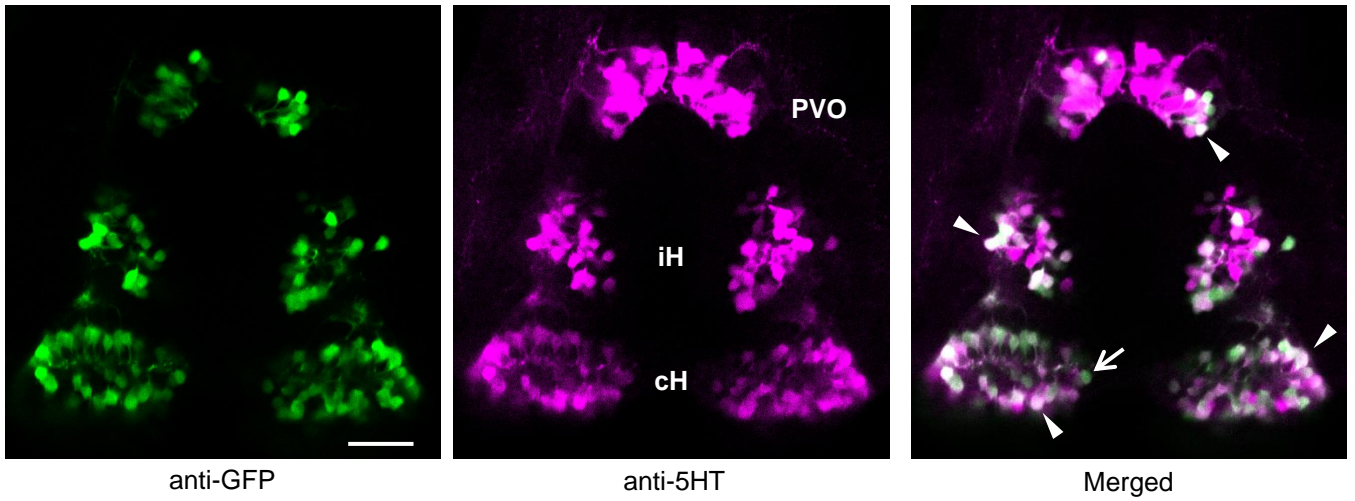
A: ROIs used for analysis. Scale bar represents 75 μm .

B: Activity of 1121A-neurons in the cH in response to mustard oil in 5 dpf 1121A-gal4; UAS:GCaMP6s larvae embedded in agarose. Graph shows the average normalized GCaMP6s fluorescence intensity (dF/Fmin) in 1121A-neurons in the cH.

The activity of 1121A-neurons in the cH during 1 minute after addition of DMSO (vehicle) was not significantly different than activity during 1 minute before adding DMSO ($n = 3$, $P = 0.28$, paired t test). The activity of 1121A-neurons in the cH during 1 minute after addition of mustard oil was significantly higher than activity during 1 minute before adding mustard oil ($n = 3$, $*P = 0.004$, paired t test).

A

116A-gal4; UAS:GFP

**B**

1121A-gal4; UAS:GFP

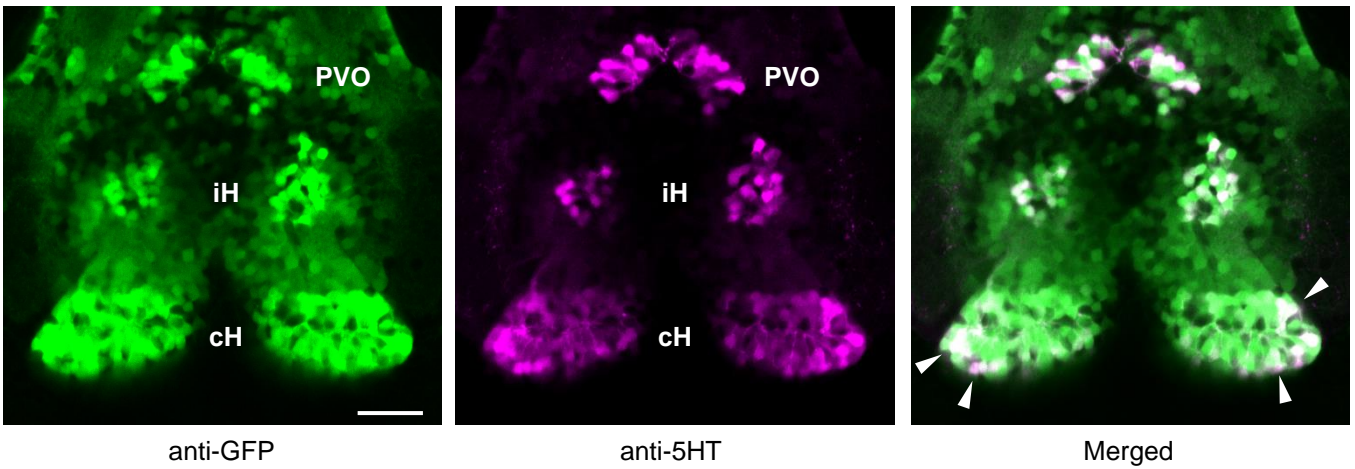


Figure 20. Immunohistochemistry of the 116A-gal4 and 1121A-gal4 lines

A-B: Overlap of GFP immunostaining (green) with 5-HT immunostaining (magenta) in cH, iH and PVO of 116A-gal4; UAS:GFP (**A**) and 1121A-gal4; UAS:GFP (**B**) larvae at 5 dpf.

Arrows show neuronal somata that express GFP but not 5-HT. Arrowheads show neuronal somata that express both GFP and 5-HT.

Scale bars represent 25 μ m.

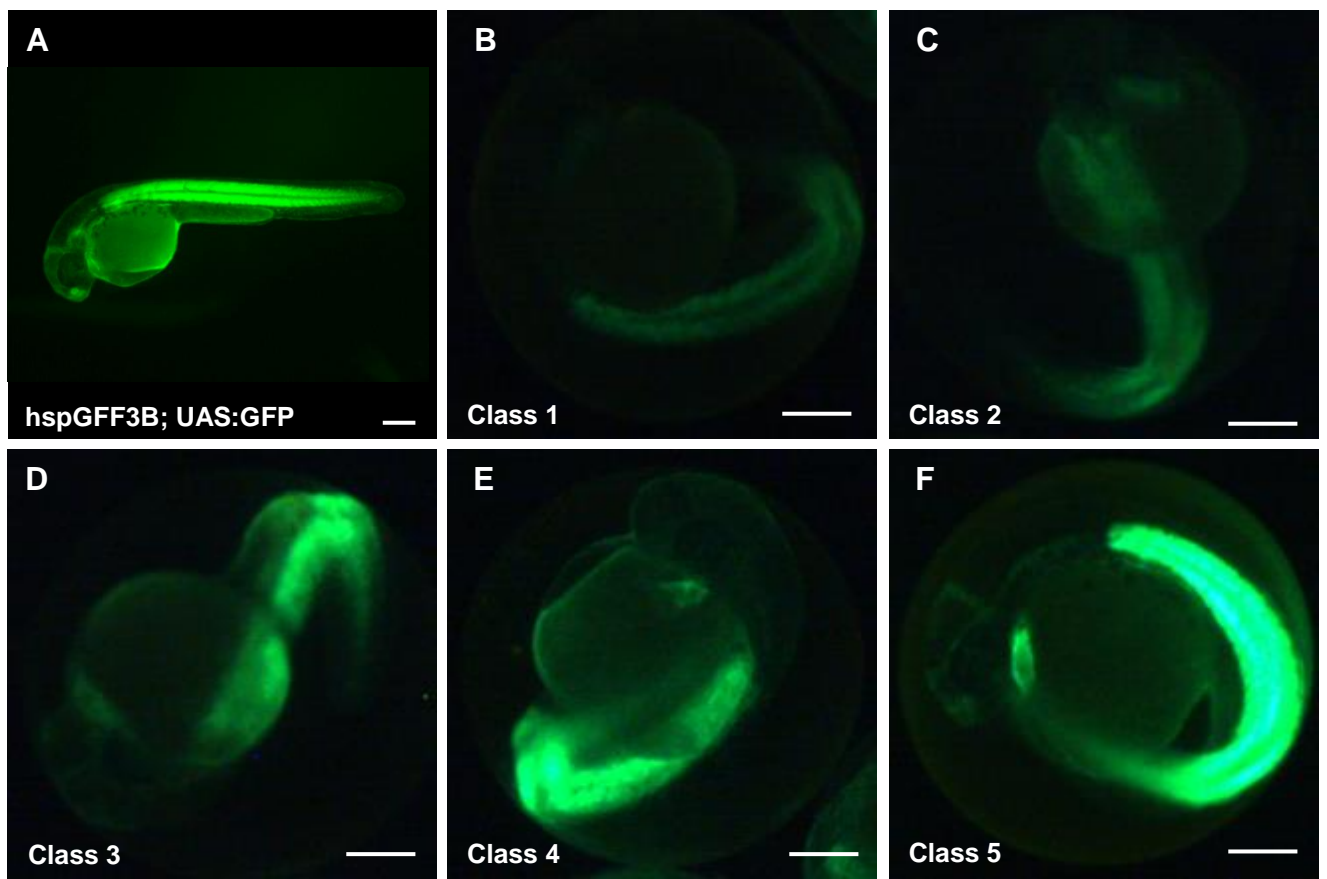


Figure 21. Establishment of a new UAS:BoTx:GFP line

A, GFP expression in hspGFF3B; UAS:GFP larvae at 5 dpf. **B-F**: representative images of hspGFF3B; UAS:BoTx:GFP embryos at 1 dpf from each class described in Table 2. Scale bars represent 200 μ m.

Table 2. Summary of founder screen for establishment of a new UAS:BoTx:GFP line

Founder	m/f	Total	GFP+	Visual			Using ImageJ Software				
				Weak	Medium	Strong	Class 1	Class 2	Class 3	Class 4	Class 5
1	m	51	1	1			1				
2	m	111	4	3	1		3	1			
3	m	22	3			3					3
4	m	136	4			4					4
5	m	80	9	2	7		1	8			
6	m	123	8	4	3	1		6	1	1	
7	m	215	67	3	3	8		3		5	6
8	m	74	16	9	5	2		4	10	2	
9	f	35	8	8			8				
10	f	83	10	2		8	1	1		4	4
11	f	80	10		8	2	4	4	1	1	
12	f	162	10		7	3		6	4		
13	f	104	9	2	3	4	2		3	4	
14	f	68	11		11			2	9		
15	f	22	2		2				2		
16	f	265	21	2	18			4	16		